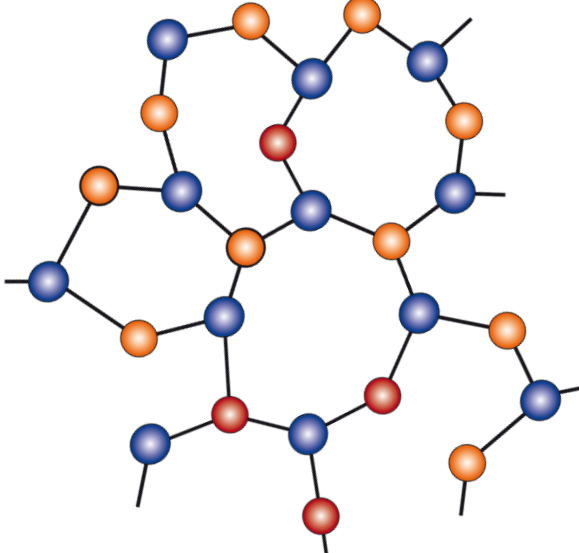
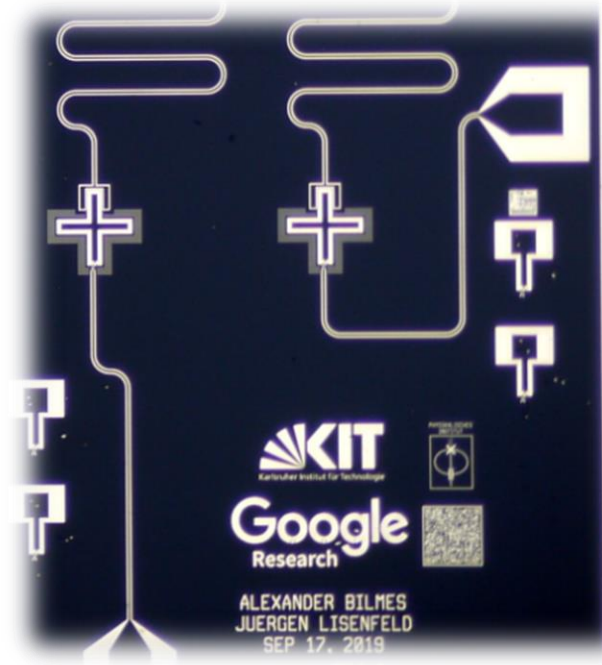


Material Defects in Superconducting Quantum Bits: Origins and Remedies

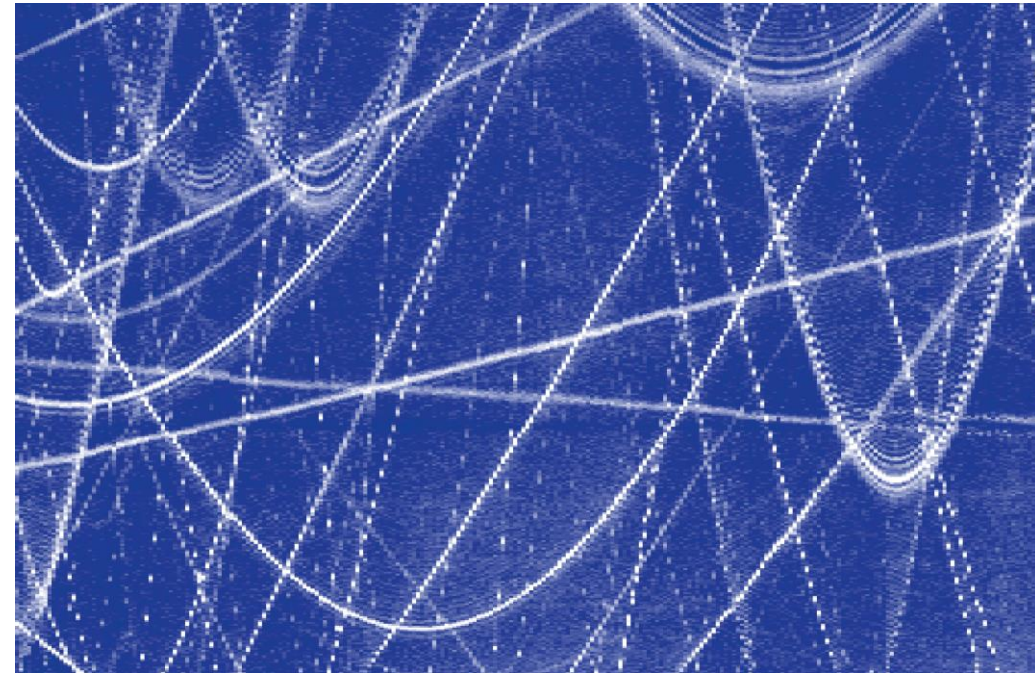
Jürgen Lisenfeld



Exploring the mysteries of glasses...



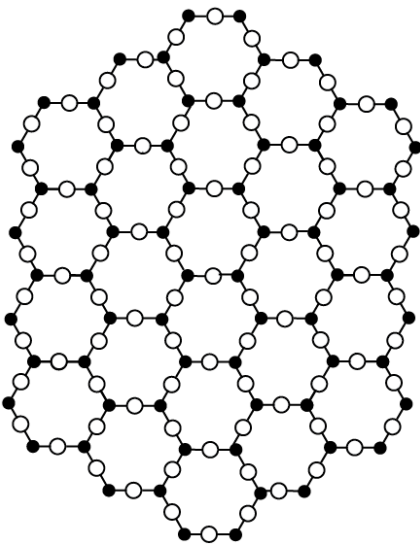
..and the sources of decoherence
in superconducting qubits...



..to shed new light on atomic tunneling defects.

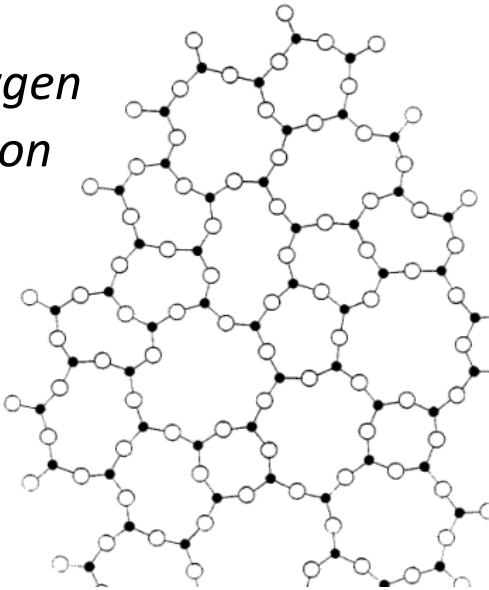
mysterious anomalies of amorphous materials

cristalline SiO_2 ('quartz')



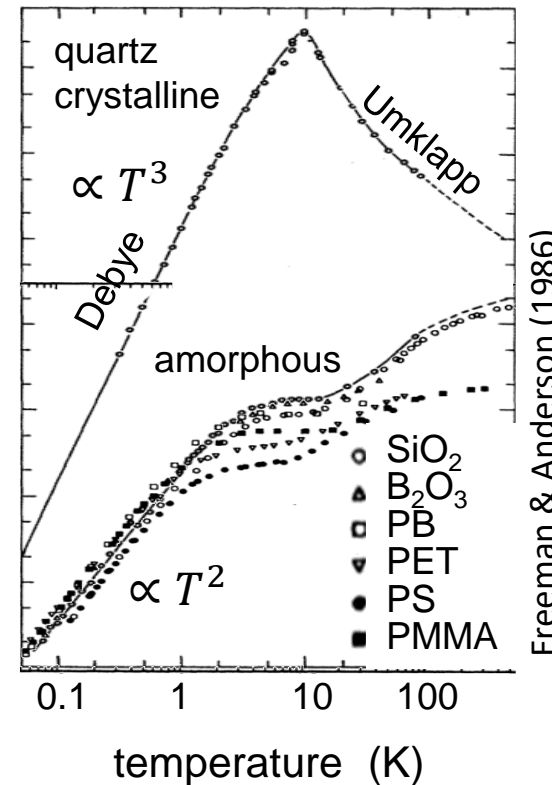
amorphous SiO_2 ("glass")

○ oxygen
● silicon

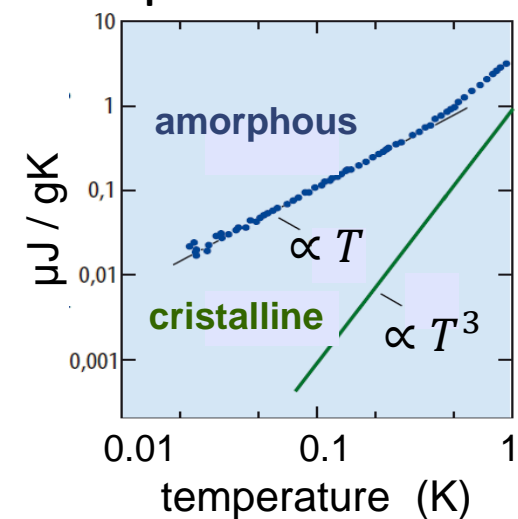


measurements in the 1970s revealed universal anomalies of glasses

thermal conductivity



specific heat



glasses must contain intrinsic states

The Standard Tunneling Model

Anderson, Halperin, Varma (1973); Phillips (1973)

- glasses contain intrinsic states

- (possibly) formed by atoms which can tunnel between two nearly equivalent positions

- model by Two-Level Tunneling Systems (TLS)

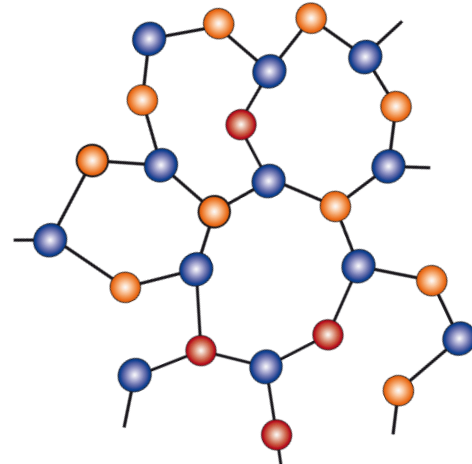
$$\hat{H}_{\text{TLS}} = \frac{1}{2} \Delta_0 \hat{\sigma}_x + \frac{1}{2} \varepsilon \hat{\sigma}_z$$

asymmetry $\varepsilon_0 + \vec{p} \cdot \vec{E} + \vec{\gamma} \cdot \vec{S}$
 el. dipole moment \vec{p}
 E-field \vec{E}
 strain $\vec{\gamma}$
 deformation potential S

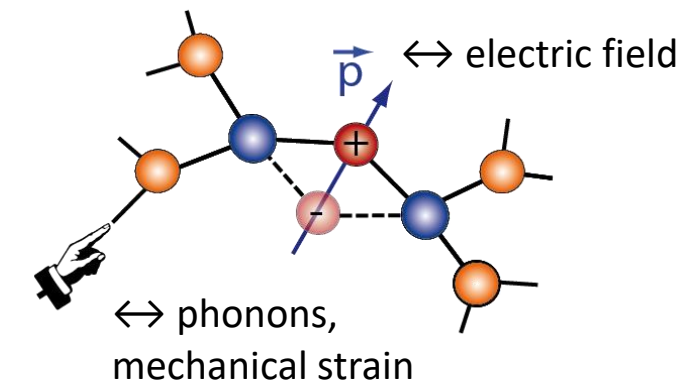
- expect constant energy distribution

$$P(E) = P_0 \approx 1000 / \text{GHz } \mu\text{m}^3$$

- neglects interactions between defects

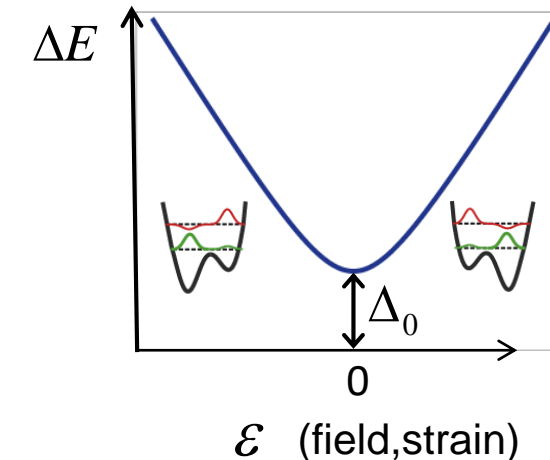
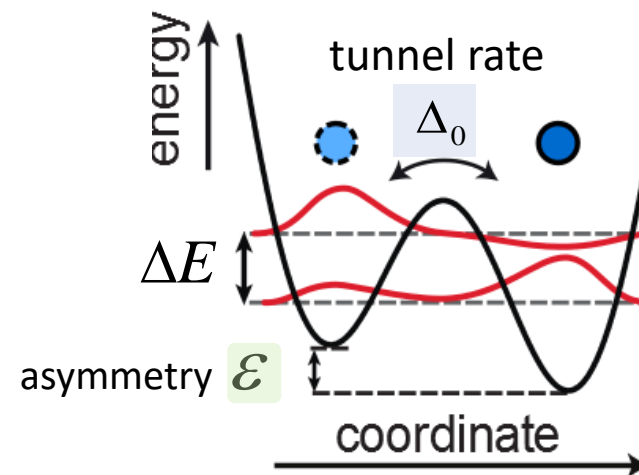


- interaction with strain & electric field



- transition energy:

$$\Delta E = \sqrt{\Delta_0^2 + \varepsilon^2}$$



TLS relaxation dynamics

■ relaxation rate

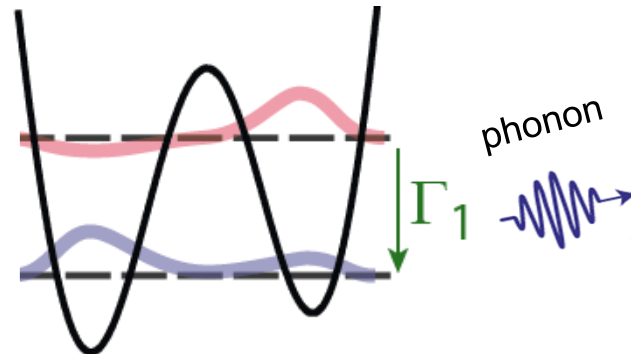
$$\Gamma_1 = \left(\frac{\gamma_l^2}{v_l^5} + 2 \frac{\gamma_t^2}{v_t^5} \right) \frac{\Delta_0^2 E}{2\pi\rho\hbar^4} \coth(E/2k_B T)$$

γ : phonon coupling strength

v : sound velocity

ρ : material density

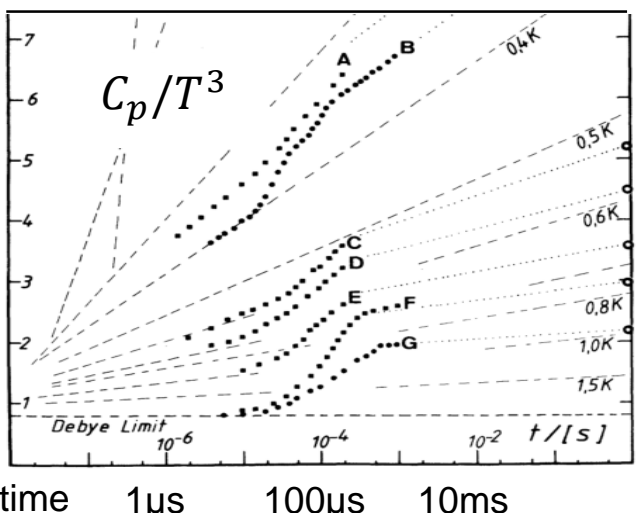
p : electric dipole moment



- ➡ • **internal friction** $Q^{-1} = \pi P_0 \gamma^2 / 2\rho v^2$
- ➡ • **dielectric loss** $\tan \delta = \pi P_0 p^2 / 6\epsilon_0 \epsilon_i$

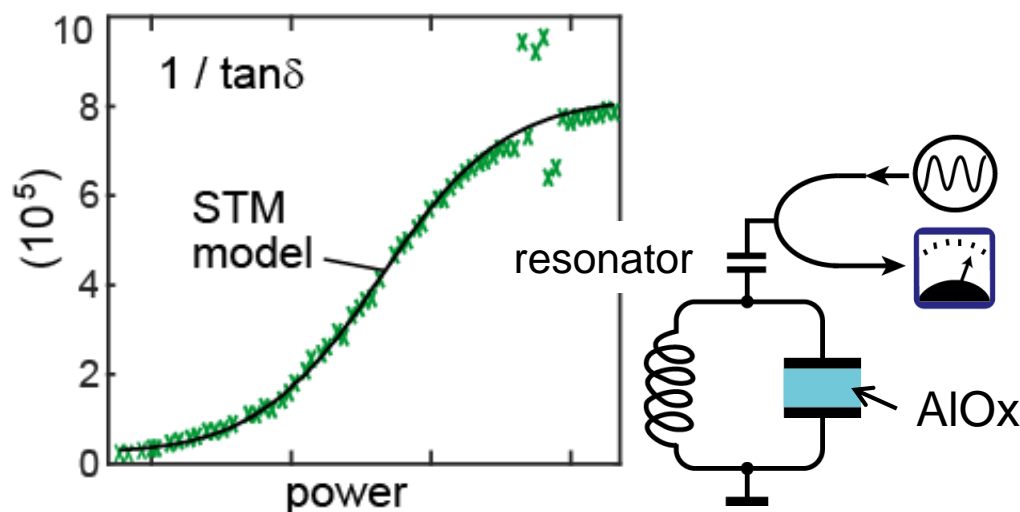
➡ specific heat depends on time

Meissner and Spitzmann, PRL 46, 265 (1981)



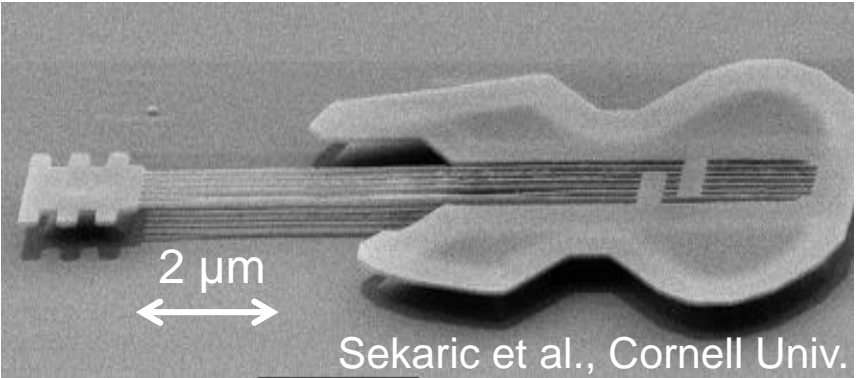
➡ Dielectric loss depends on power

J.D. Brehm, J. Lisenfeld et al., APL 111, 12601 (2017)



Devices affected by TLS defects

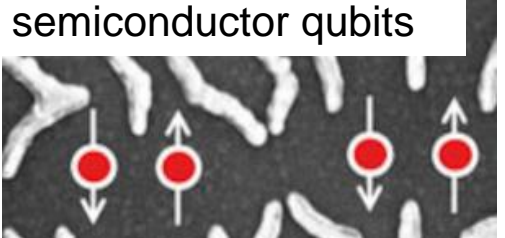
■ nanomechanical resonators



■ quantum systems ion trap (Los Alamos)



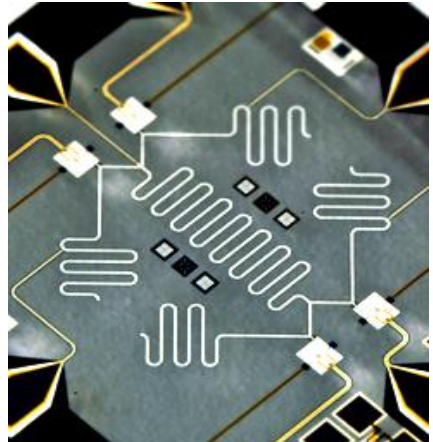
semiconductor qubits



5

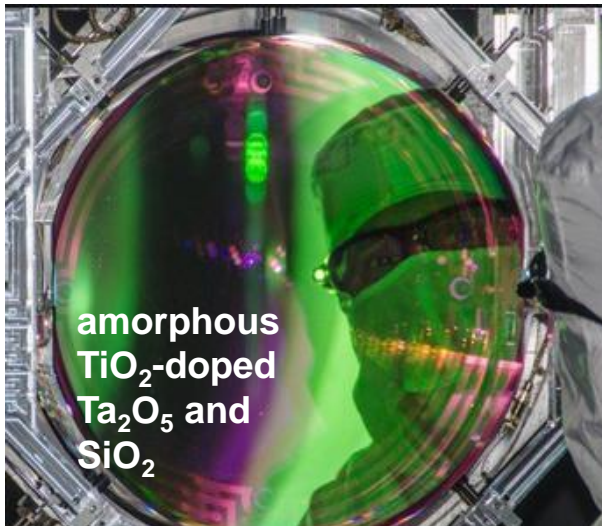
Bluhm, RWTH Aachen

■ superconducting qubits



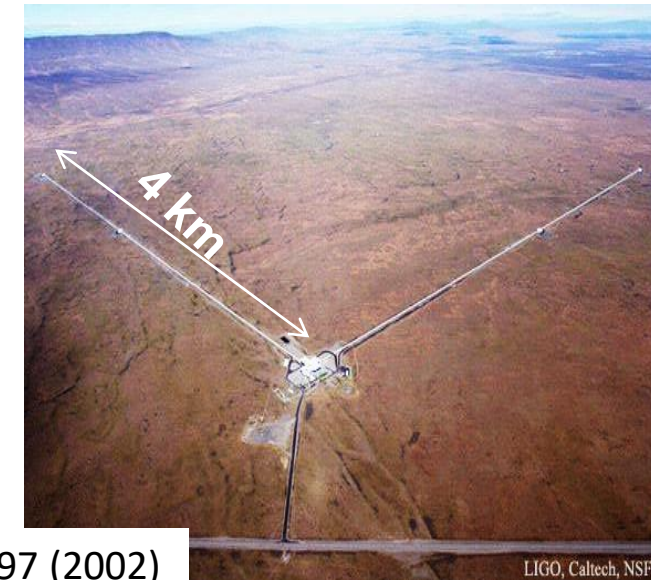
Martinis Group, UCSB

■ optical cavities (Lasers, LIGO, ...)



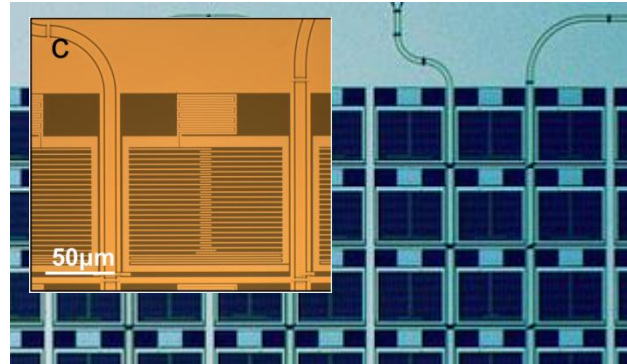
amorphous
 TiO_2 -doped
 Ta_2O_5 and
 SiO_2

Harry et al., Class. Quant. Grav. 19, 897 (2002)



LIGO, Caltech, NSF

■ kinetic inductance detectors



Dodkins et al., 2018

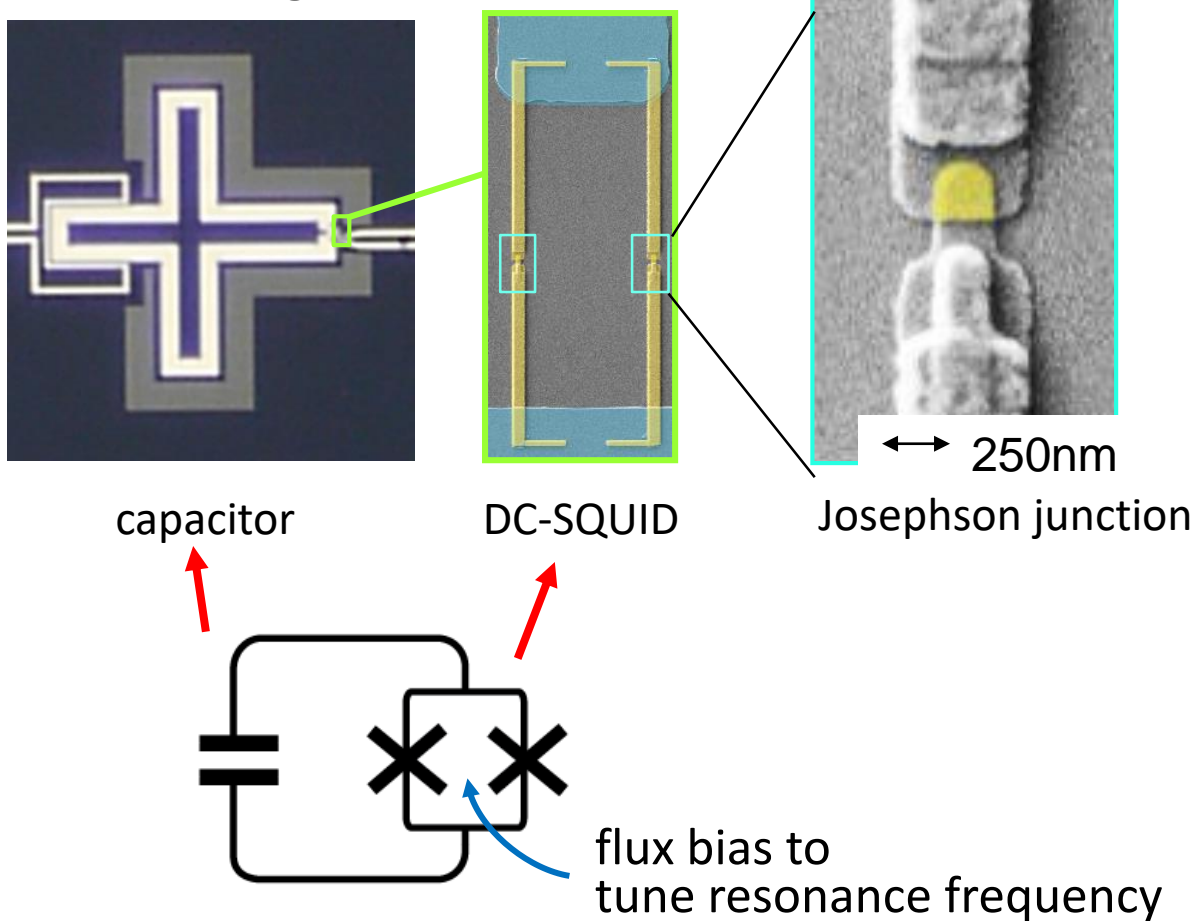
■ accelerator cavities



Romanenko et al., PRL 119 (2017)

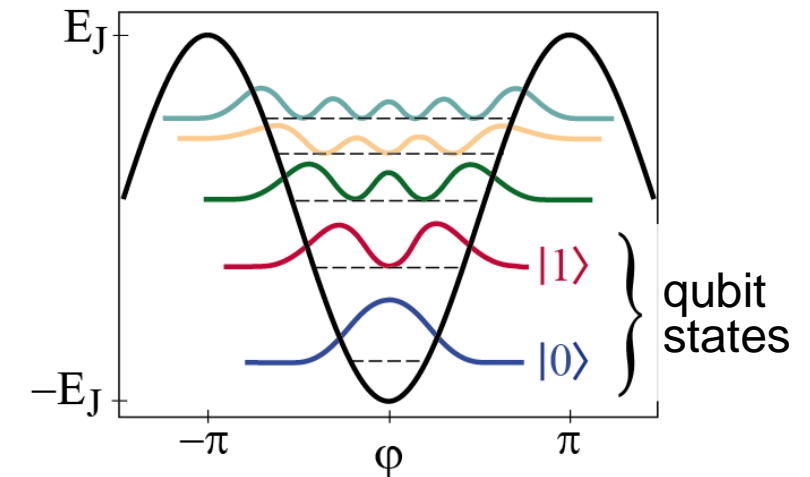
Transmon Qubits

- „Xmon“ design R. Barends et al. (2013)



Qubits are non-linear LC-Resonators

- Transmon qubit energy levels



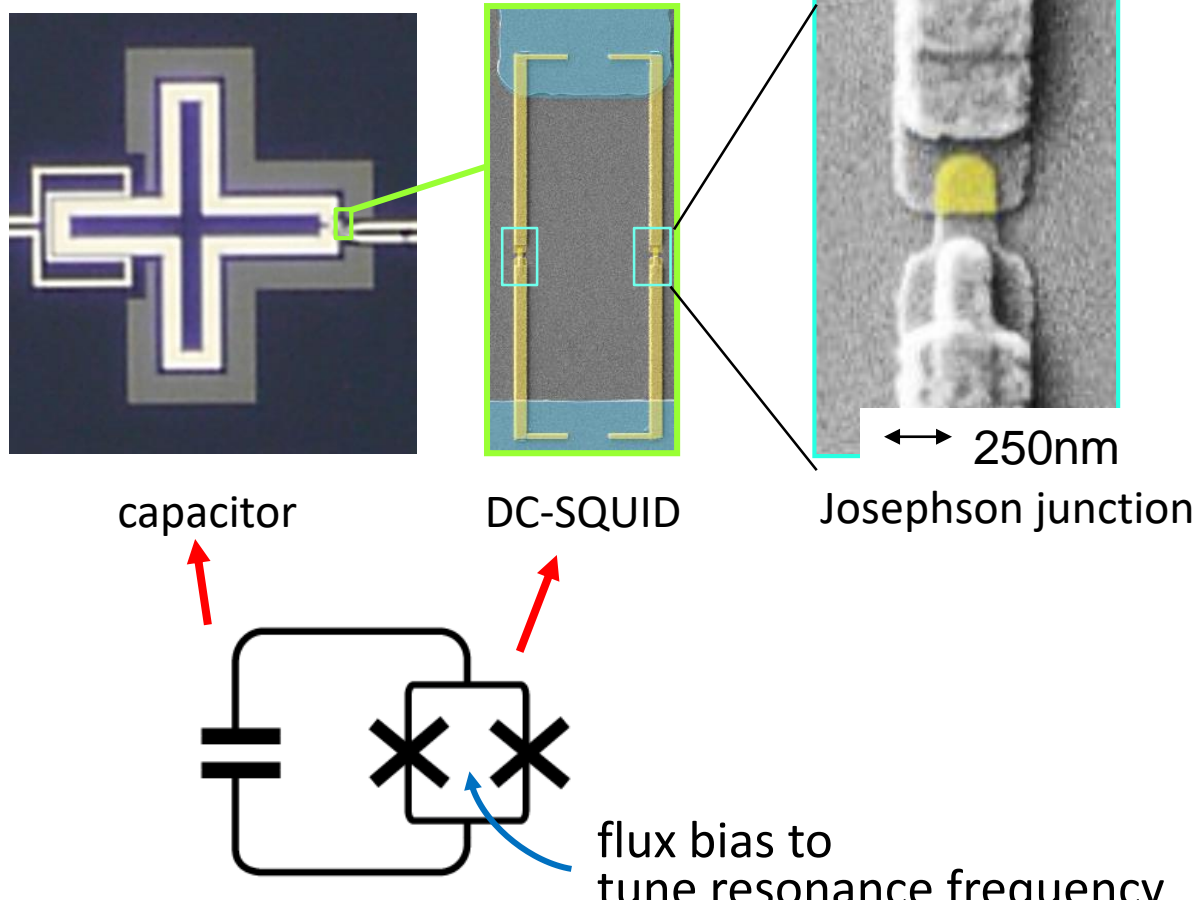
$$\hat{H} = \frac{\hat{Q}^2}{2C} - E_J \cos \varphi$$

$$E_J = \frac{\eta I_c}{2e}$$

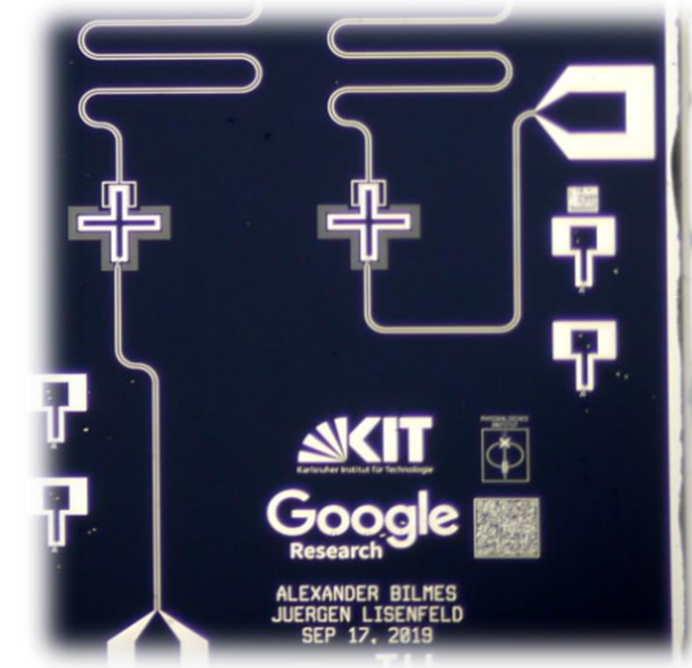
Transmon Qubits

■ Transmons made at KIT (A. Bilmes)

■ „Xmon“ design R. Barends et al. (2013)



Qubits are non-linear LC-Resonators

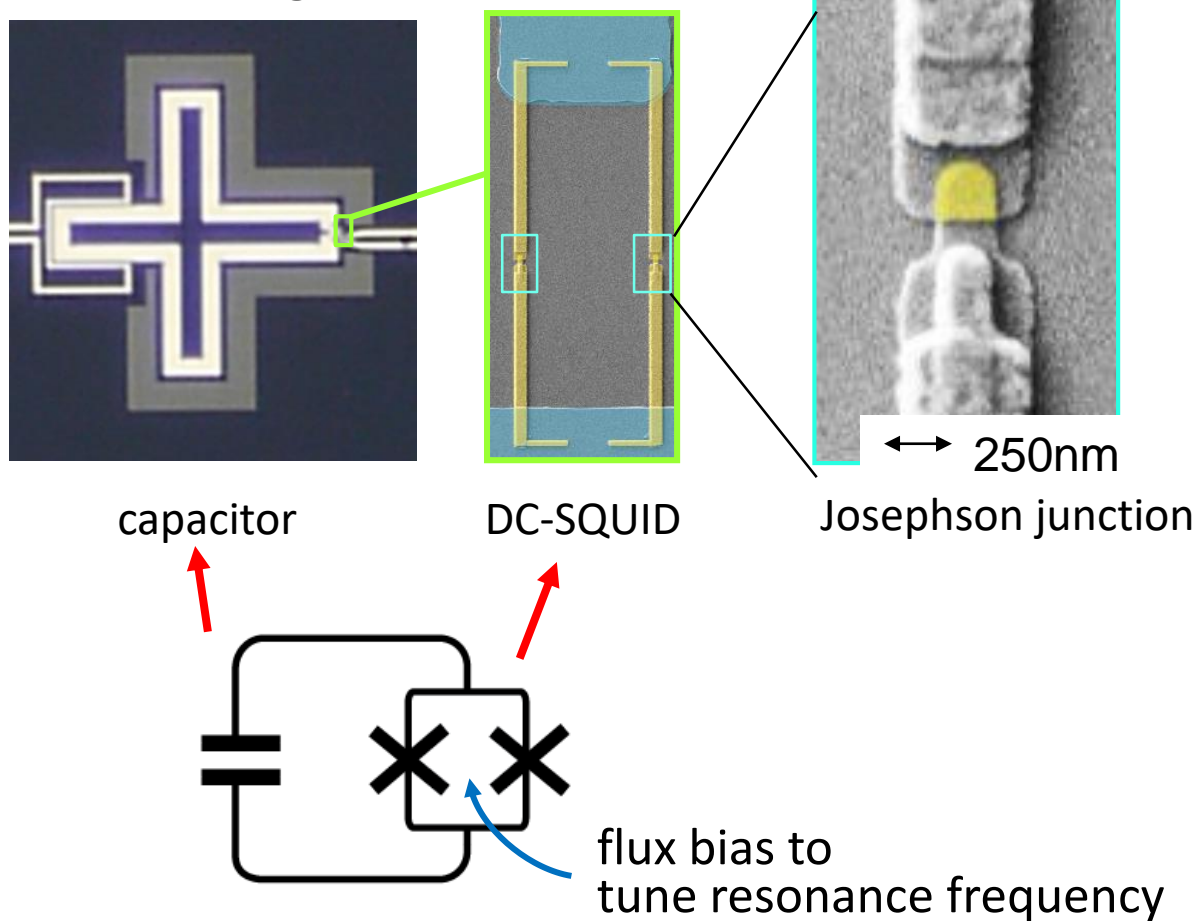


■ 433-qubit processor made by IBM



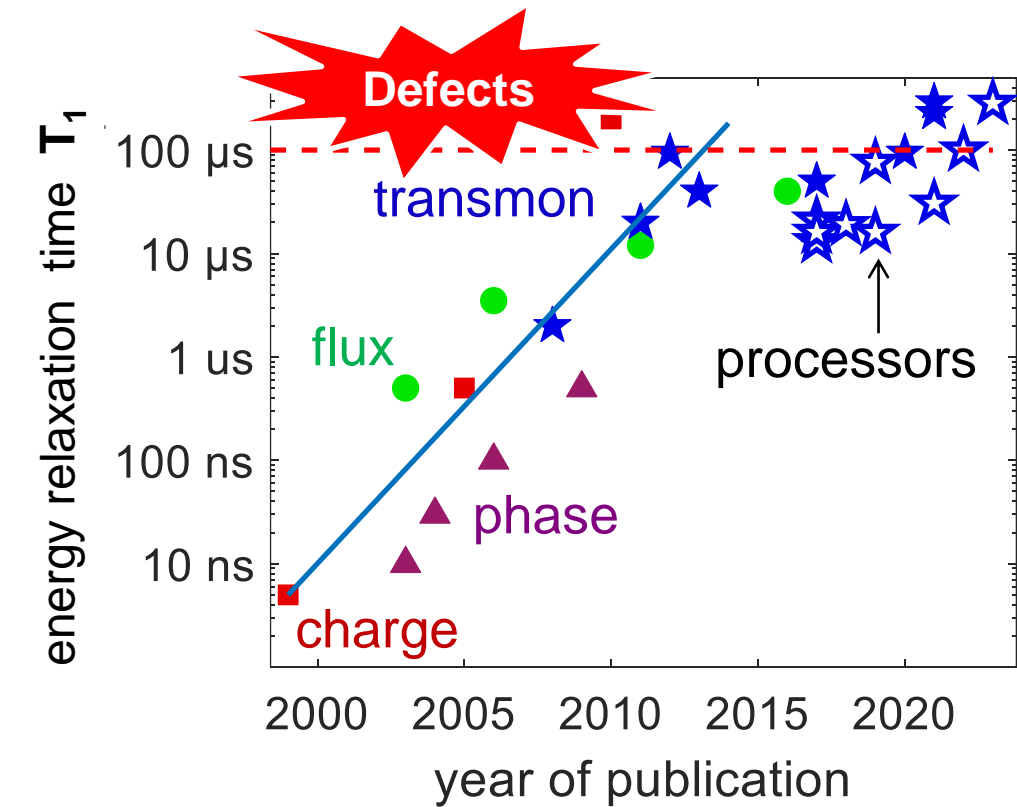
Transmon Qubits

- „Xmon“ design R. Barends et al. (2013)



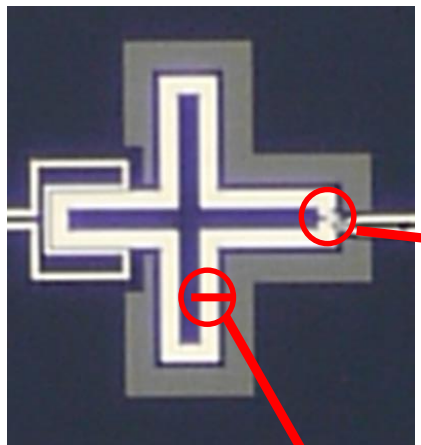
Qubits are non-linear LC-Resonators

- qubit coherence is limited by material defects

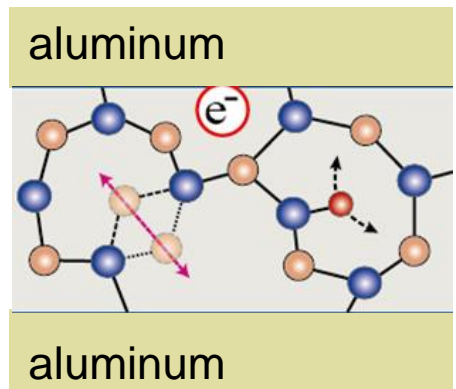


Material Defects in Qubits

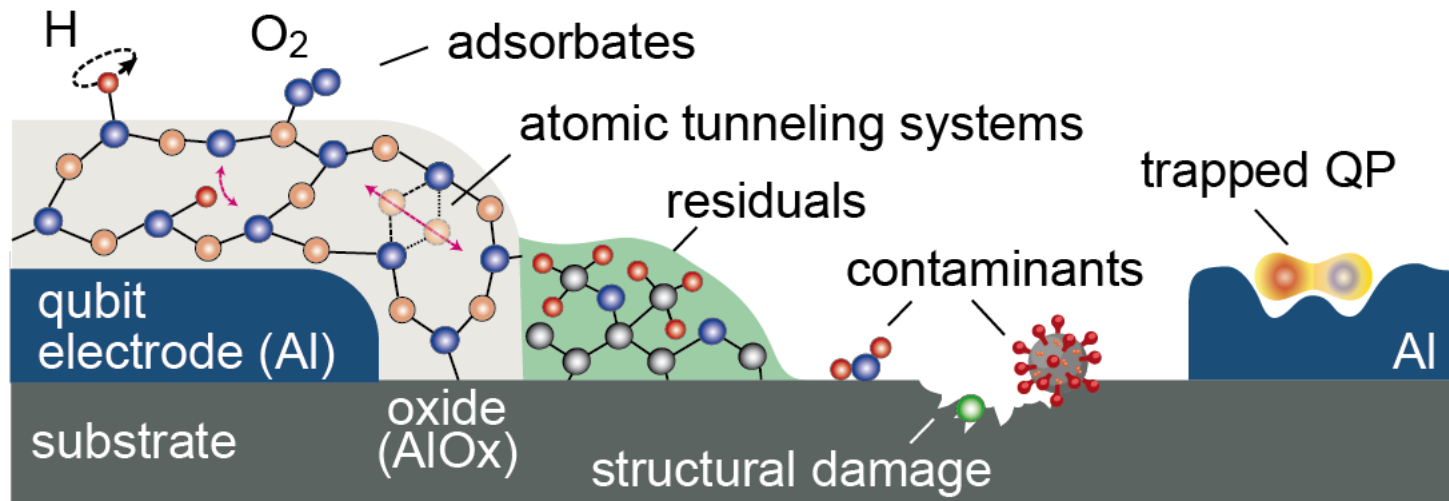
Transmon qubit



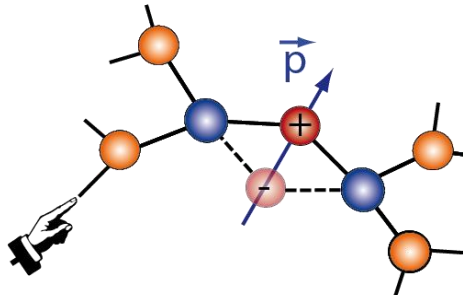
Josephson junction



circuit surface



- **TLS couple to the AC-electric field of the qubit mode**



- **TLS have random resonance frequencies**

Defect Models

Tunneling atoms

W.A. Phillips, Rep. Prog. Phys. **50**

Hydrogen rotors and interstitials

A.M. Holder et al., PRL **111**
Zhe Wang et al., PRB **98**

Andreev fluctuators

L. Faoro, L.B. Ioffe et al., PRL **95**
R. de Sousa et al., PRB **80**

Kondo resonances

L. Faoro, L.B. Ioffe, PRL **96**

Metal-induced gap states

S.K. Choi et al., PRL **103**

Phonon-dressed electrons

K. Agarwal et al., PRB **87**

Trapped Quasiparticles

S. deGraaf et al., Sci. Adv. **6**

physisorbed Hydrogen + O₂

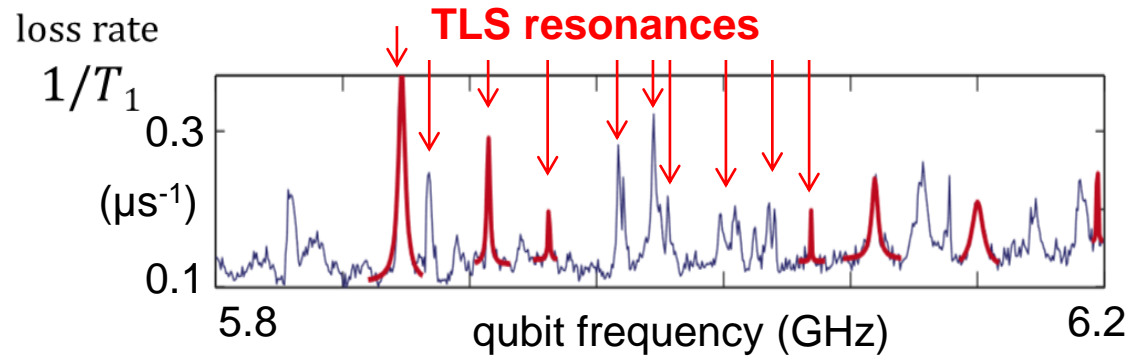
S. deGraaf et al., PRL **118**,
Nature Comm. **9** (2018)

Review:

C.Müller, J.Cole, J.Lisenfeld,
Rep. Prog. Phys. **82**, 24501 (2019)

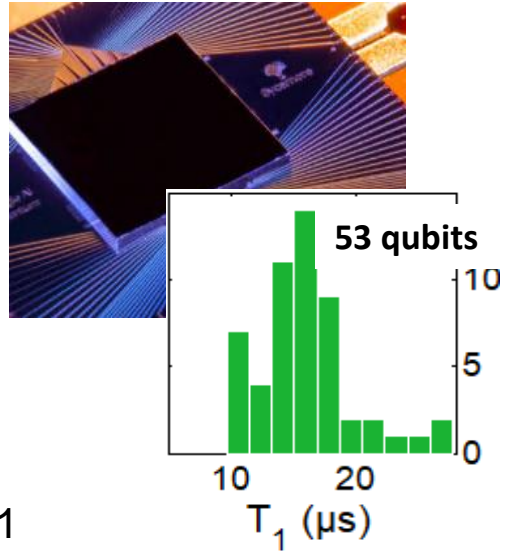
How TLS defects spoil qubit coherence

T_1 depends on qubit frequency

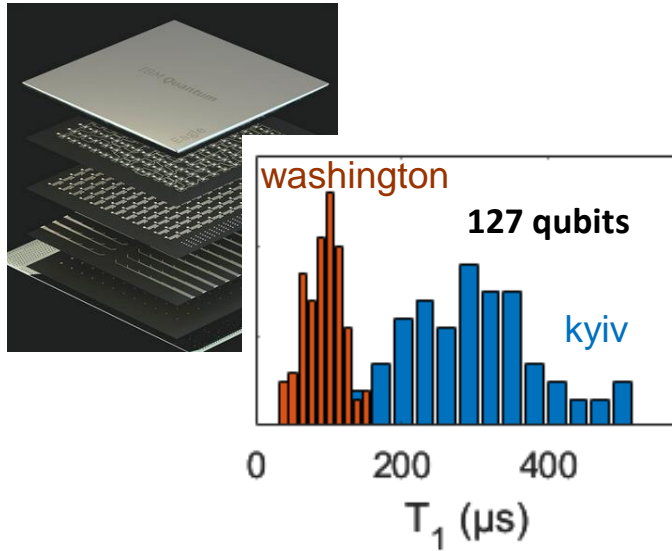


T_1 depends on the sample

- **Sycamore** (Google)
F. Arute et al., nature (2019)

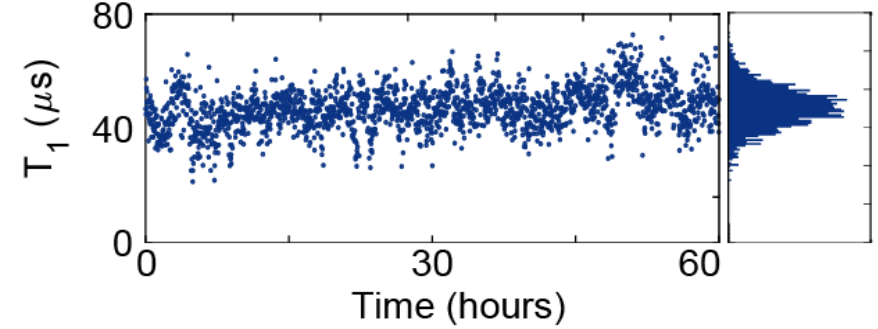


- **Eagle** (IBM, 2022)
<https://quantum-computing.ibm.com>



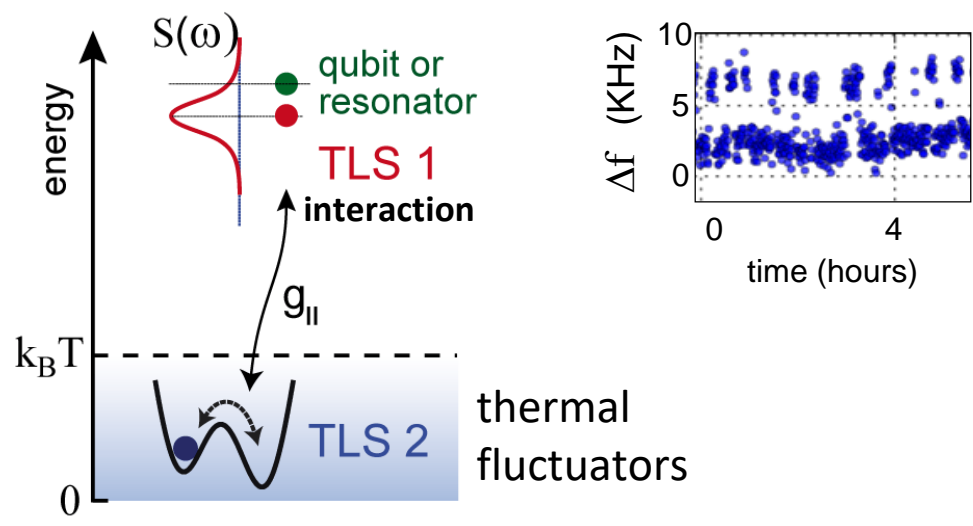
T_1 depends on time

J.J. Burnett et al., npj Quant. Inf. 5 (2019)



→ Interaction with thermal fluctuators

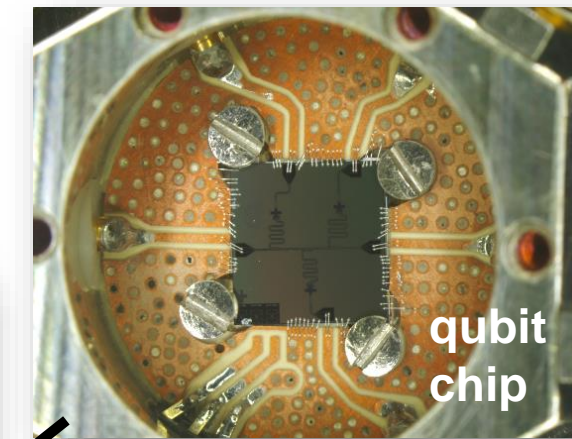
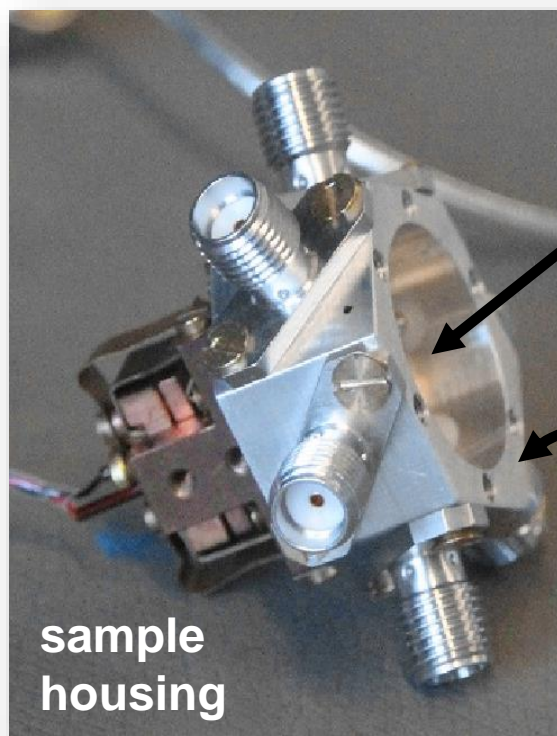
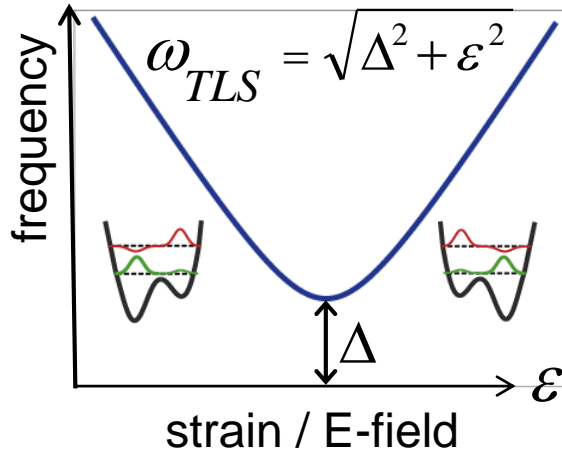
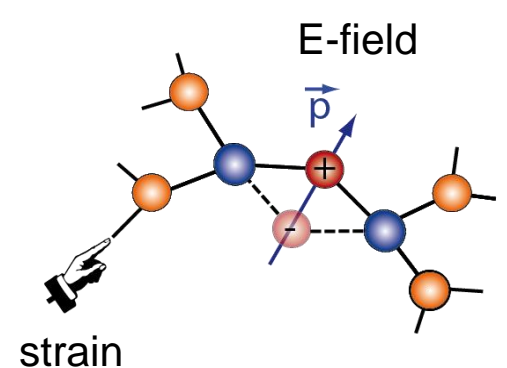
- L. Faoro, L. Ioffe, PRB 91, 014201 (2014)
- C. Müller, J.L. et al., PRB 92, 035442 (2015)
- S. Schlör, J.L. et al., PRL 123, 190502 (2019)



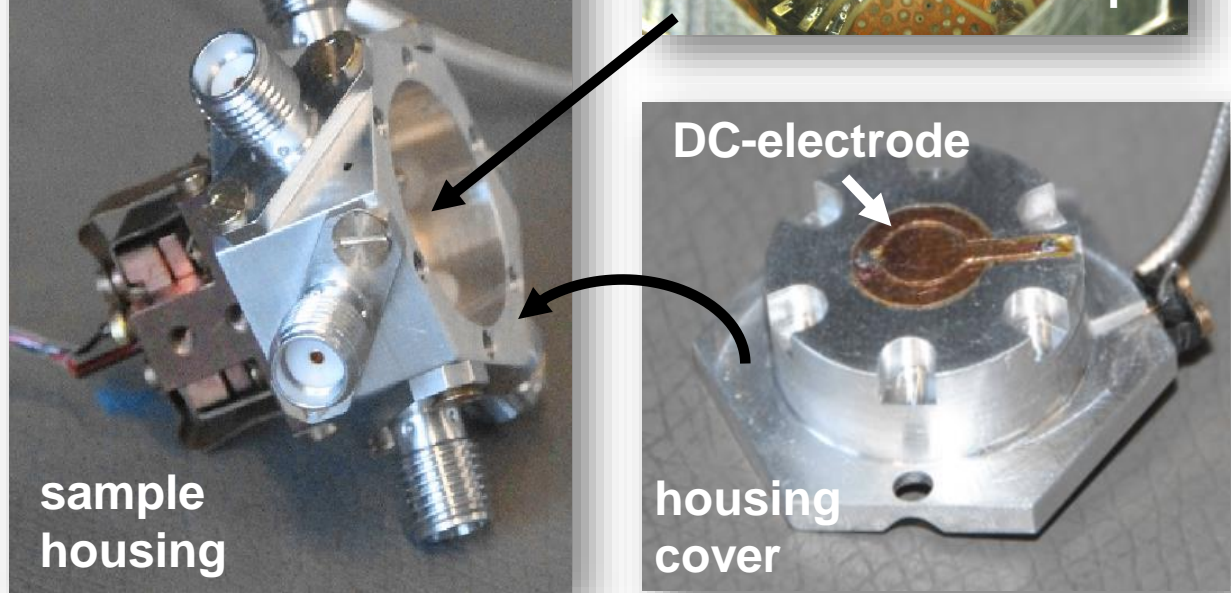
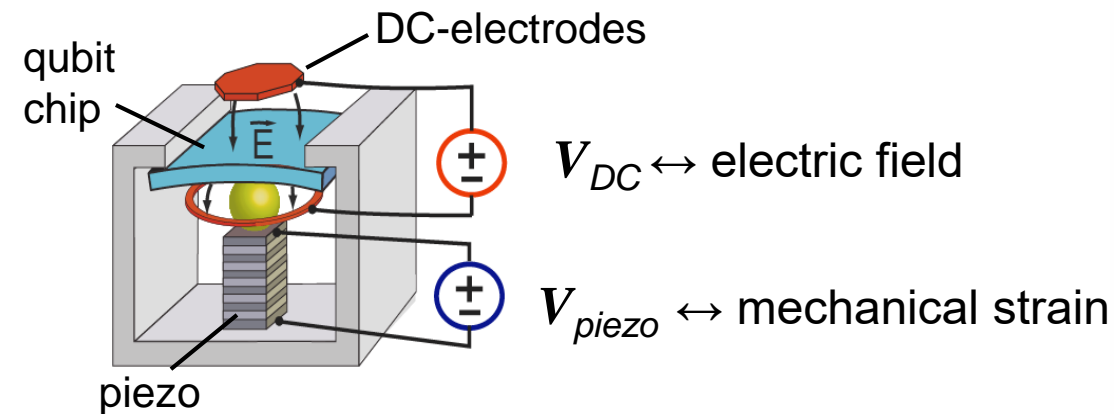
controlling TLS by mechanical strain and electric fields

J. Lisenfeld, A. Bilmes et al.,
npj Quant. Inf. 5, 105 (2019)

■ tune TLS resonance frequency



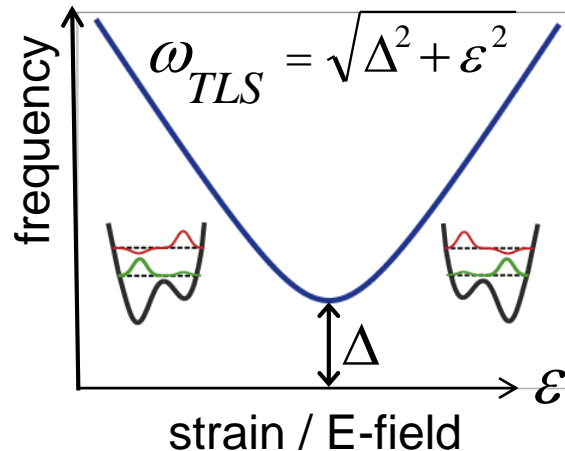
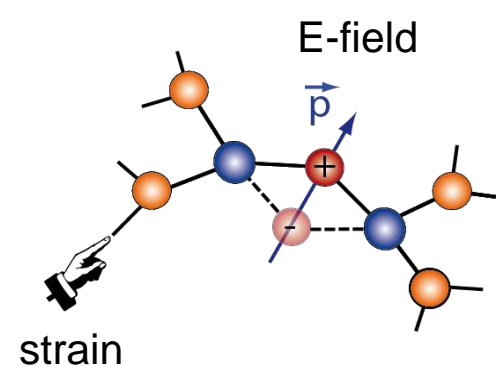
■ strain- and electric-field tuning



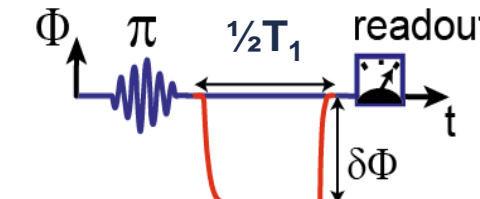
controlling TLS by mechanical strain and electric fields

J. Lisenfeld, A. Bilmes et al.,
npj Quant. Inf. 5, 105 (2019)

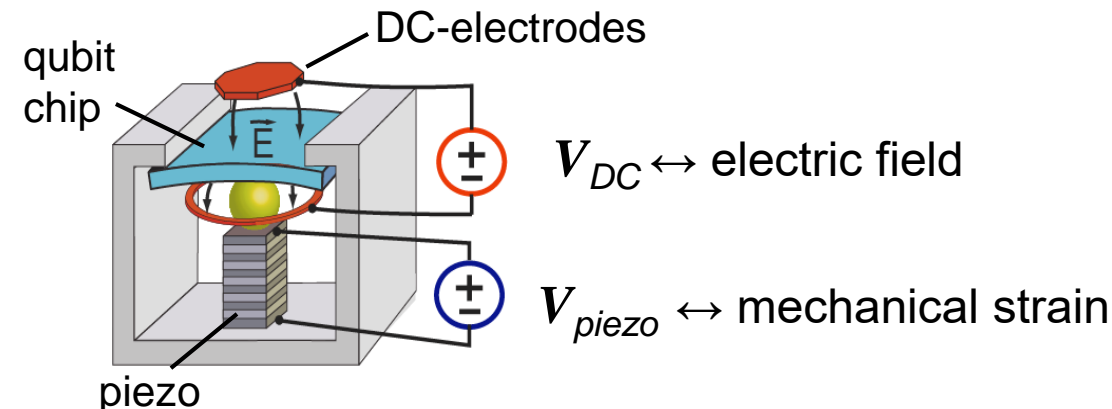
■ tune TLS resonance frequency



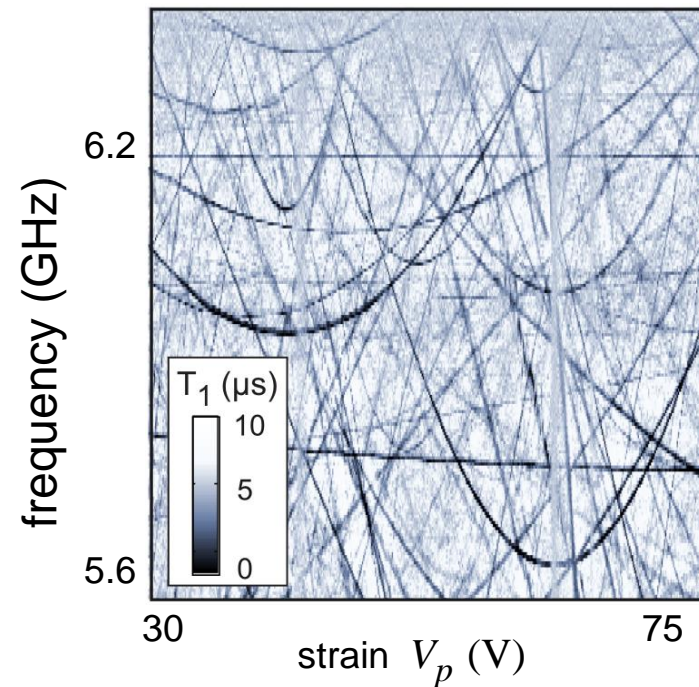
■ Detect TLS by swap spectroscopy



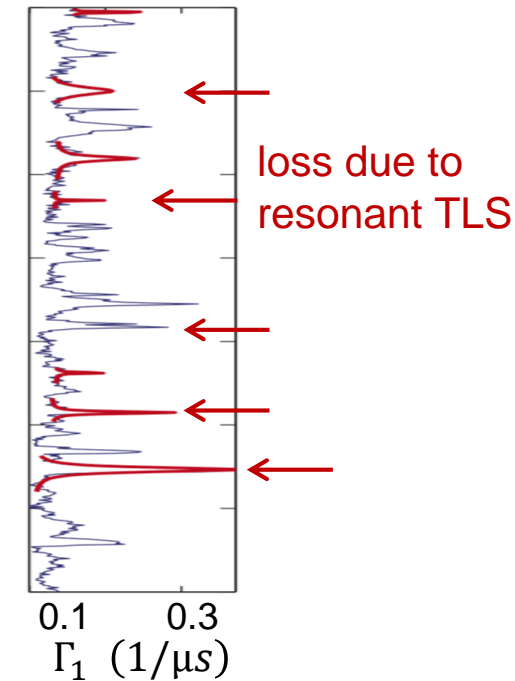
■ strain- and electric-field tuning



■ strain dependence

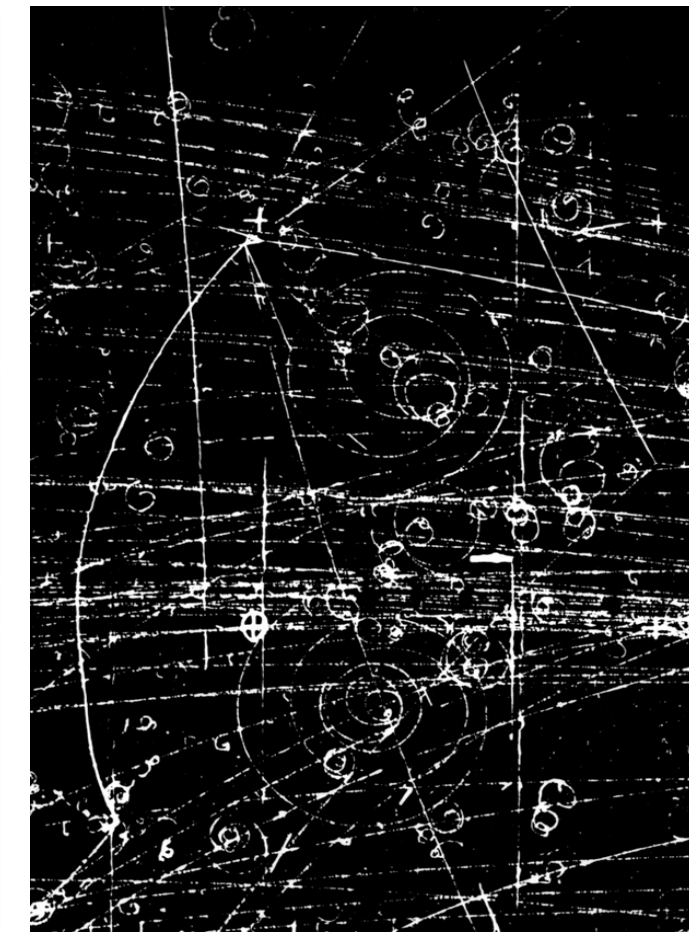
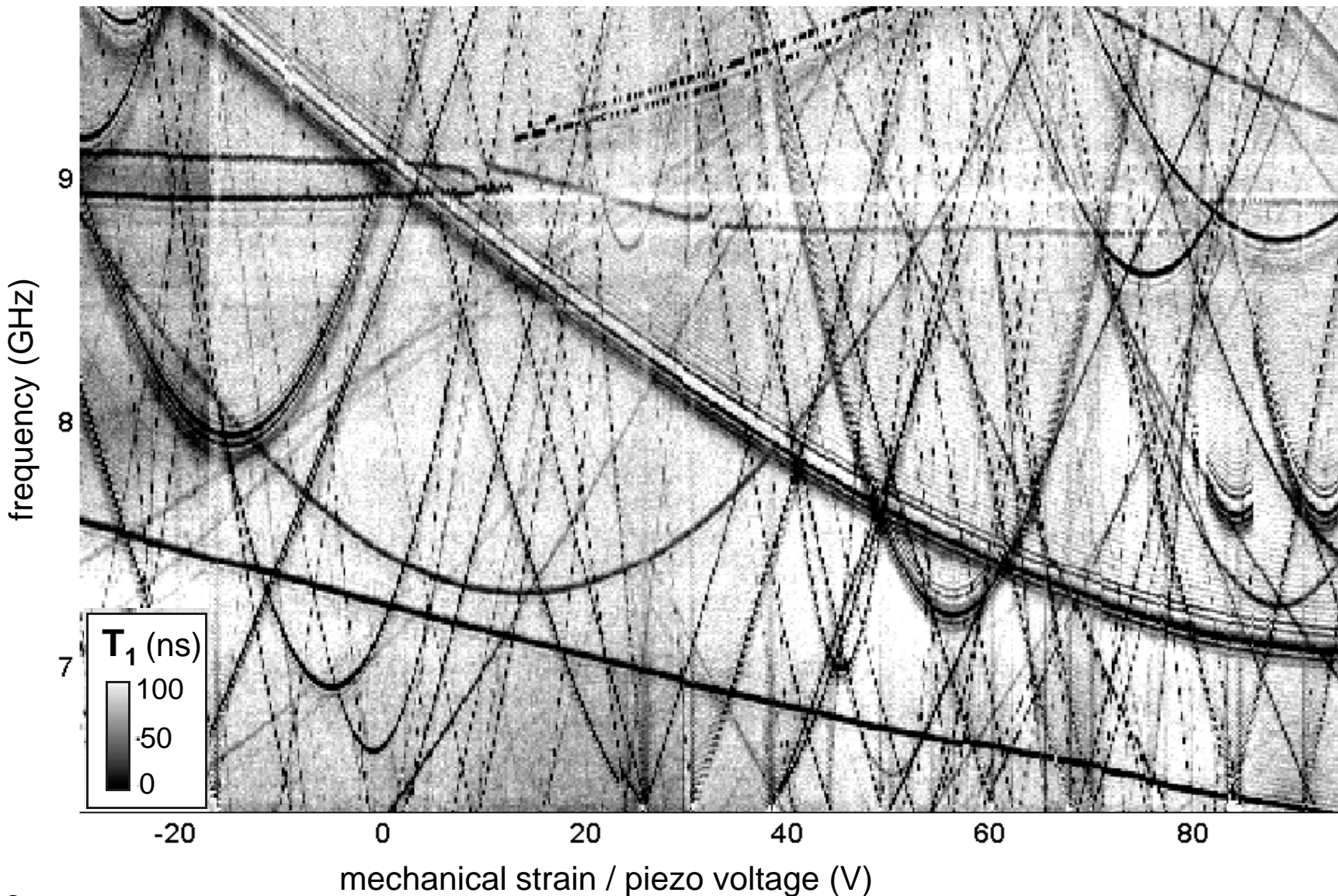


qubit loss rate



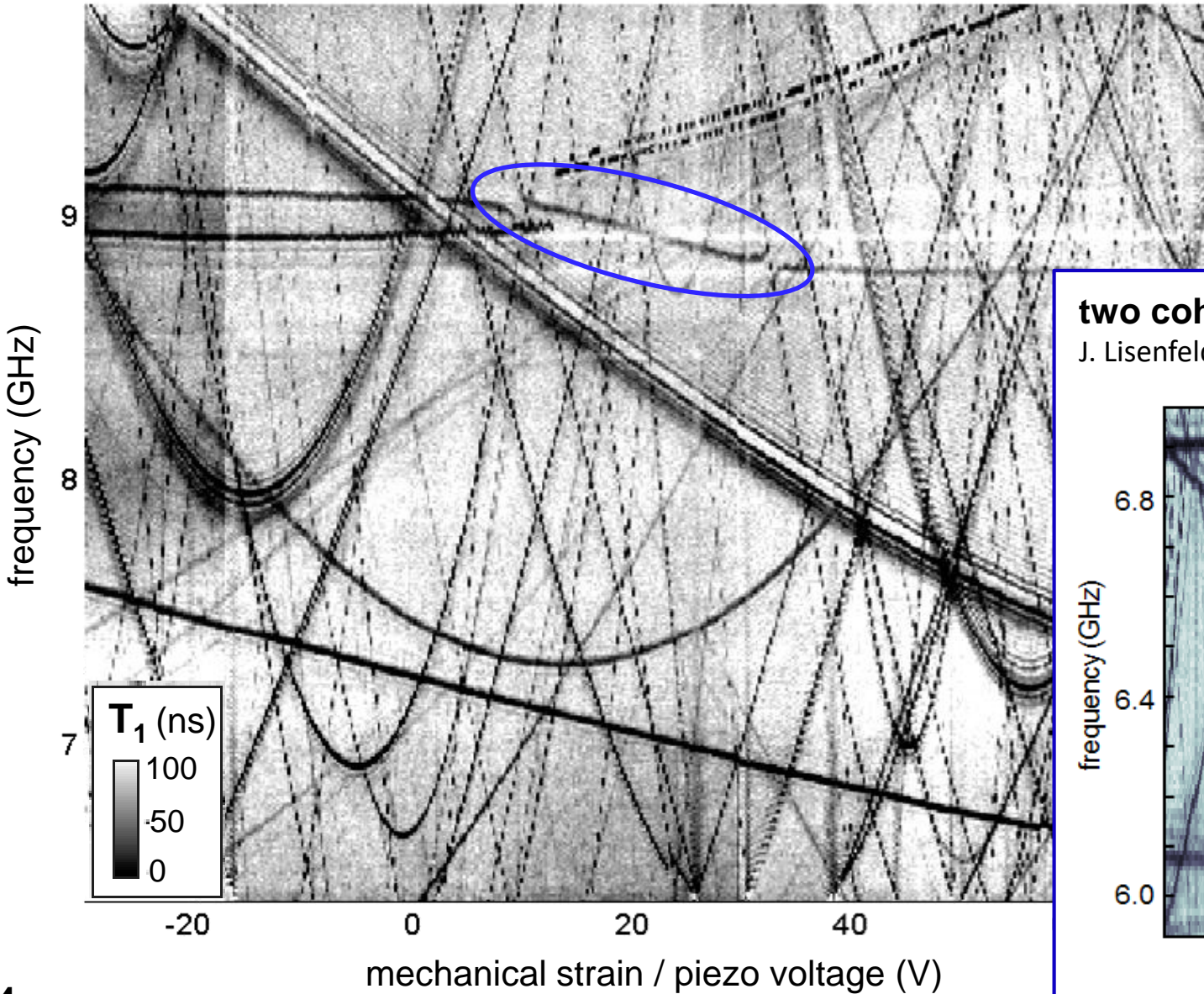
TLS strain spectroscopy

J. Lisenfeld, G. Grabovskij, C. Müller, J. Cole, A.V. Ustinov et al., Nat. Comm. 6, 6182 (2015)



Cloud chamber photograph (1958)
U.S. National Archives

TLS studies at KIT



TLS strain spectroscopy

Grabovskij et al., Science 338, 232 (2012)

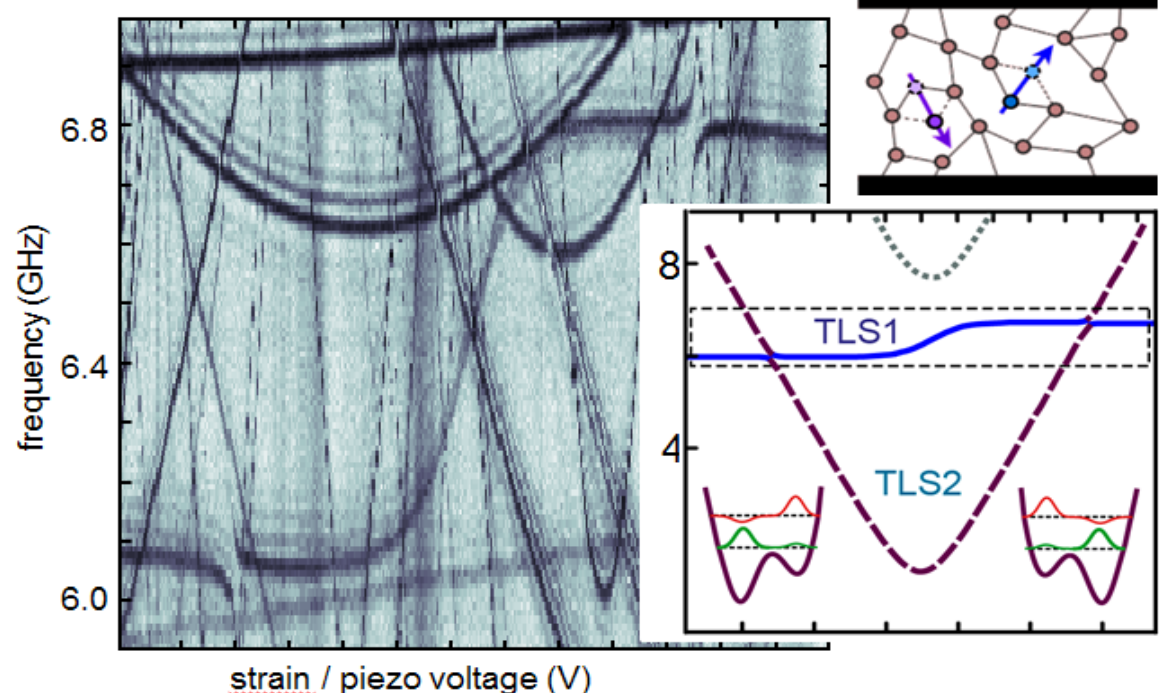
coherently coupled TLS

Grabovskij et al., NJP 13, 063015 (2011)

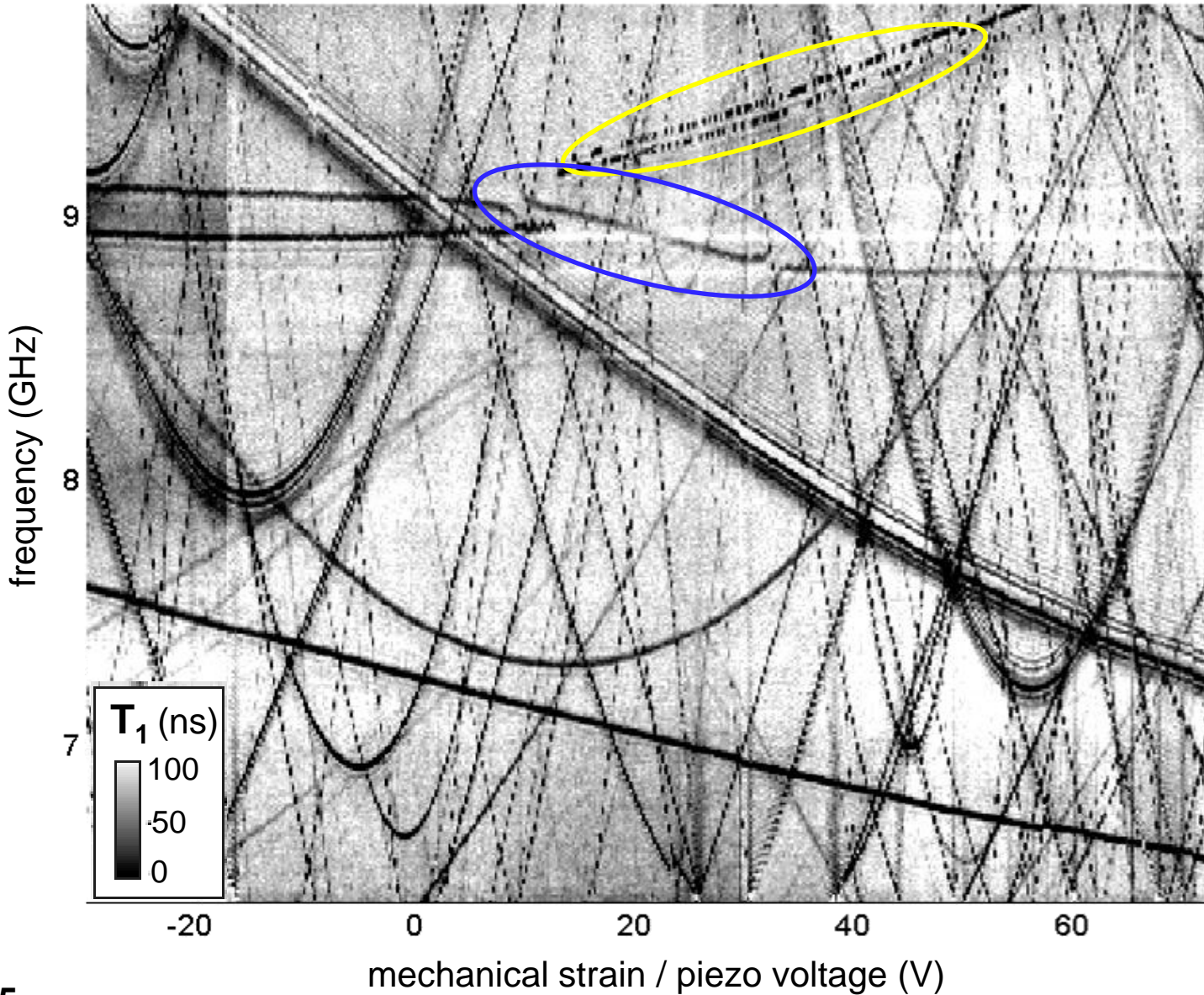
Lisenfeld et al., nature comm. 6, 6182 (2015)

two coherently coupled TLS

J. Lisenfeld et al., Nat. Commun. 6, 6182 (2015)



TLS studies at KIT



TLS strain spectroscopy

Grabovskij et al., Science 338, 232 (2012)

coherently coupled TLS

Grabovskij et al., NJP 13, 063015 (2011)

Lisenfeld et al., nature comm. 6, 6182 (2015)

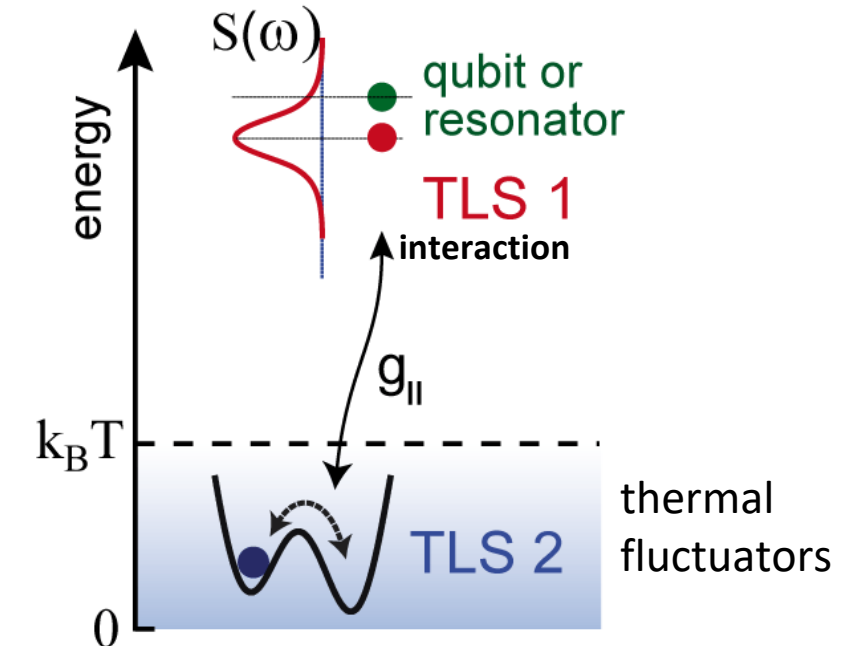
noise from thermal TLS

Müller et al., PRB 92, 035442 (2015)

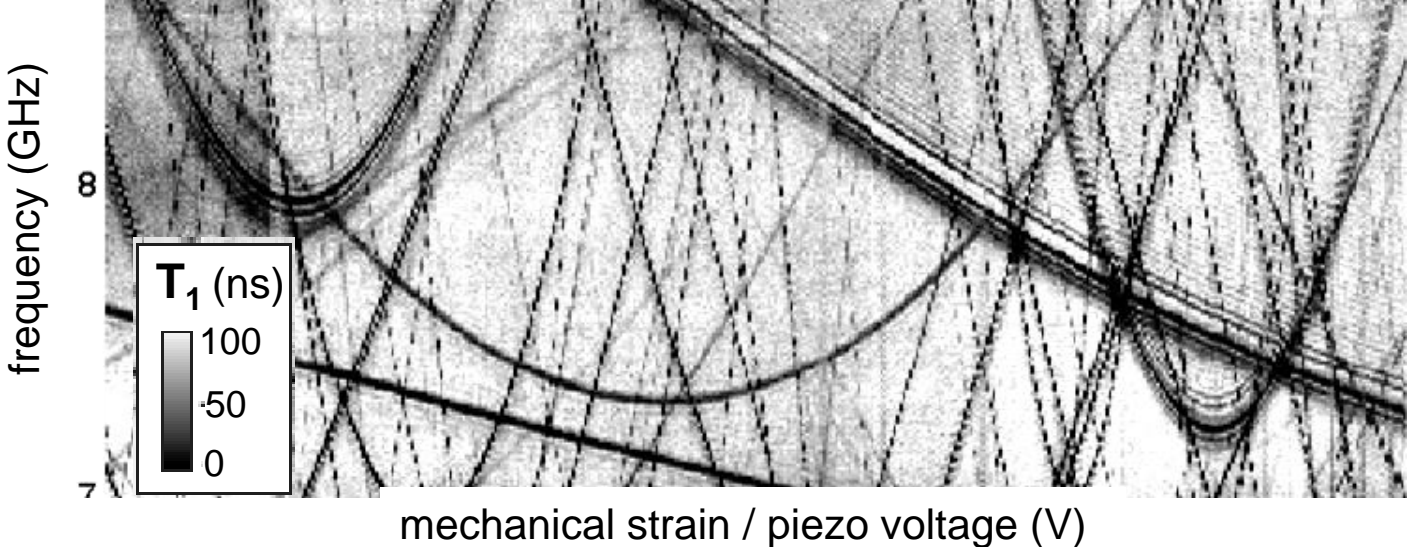
Brehm et al., APL 111, 112601 (2017)

Meissner et al., PRB 97, 180505 (2018)

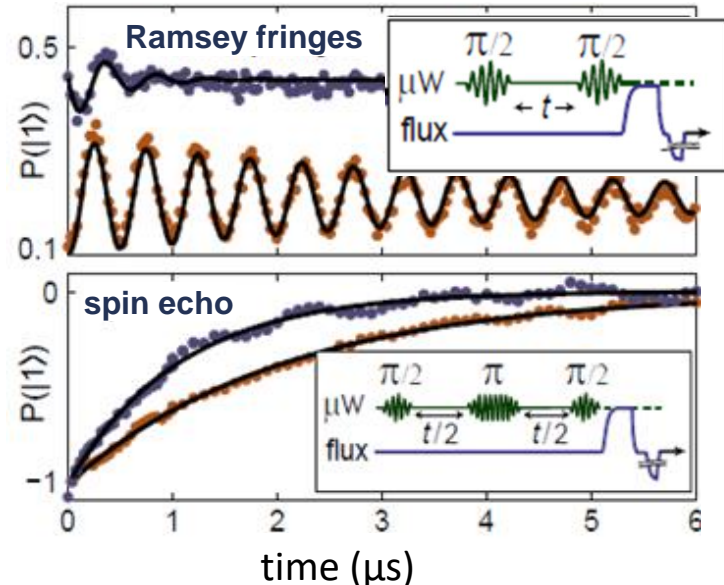
Schlör et al., PRL 123, 190502 (2019)



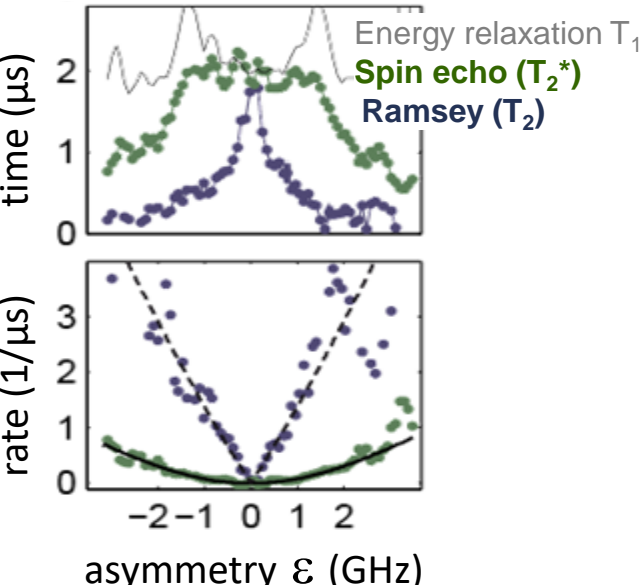
TLS studies at KIT



coherent TLS control and readout



Decoherence spectroscopy



TLS strain spectroscopy

Grabovskij et al., Science 338, 232 (2012)

coherently coupled TLS

Grabovskij et al., NJP 13, 063015 (2011)

Lisenfeld et al., nature comm. 6, 6182 (2015)

noise from thermal TLS

Müller et al., PRB 92, 035442 (2015)

Brehm et al., APL 111, 112601 (2017)

Meissner et al., PRB 97, 180505 (2018)

Schlör et al., PRL 123, 190502 (2019)

testing microscopic models

Cole et al., APL 97, 252501 (2010)

Bushev et al., PRB 82, 134530 (2010)

coherent TLS control & readout

Lisenfeld et al., PRL 12, 230504 (2010)

Lisenfeld et al., PRB 81, 100511 (2010)

Lisenfeld et al., Sci. Rep. 6, 23786 (2016)

Bilmes et al., PRB 96, 064504 (2016)

Matityahu et al., PRB 95, 241409(R) (2017)

electric-field tuning of TLS

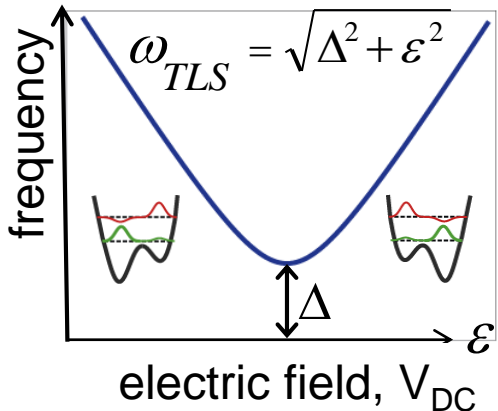
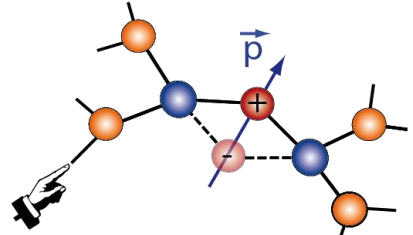
Lisenfeld et al., npj Quant. Inf. 5, 105 (2019)

Bilmes et al., Sci. Rep. 10, 3090 (2020)

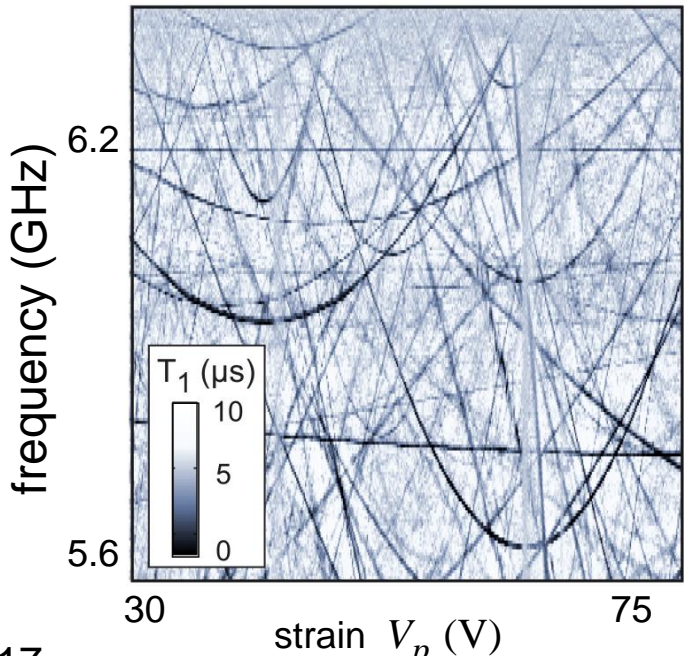
Lisenfeld et al., npj Quant. Inf. 9, 8 (2023)

Controlling defects by Electric Fields

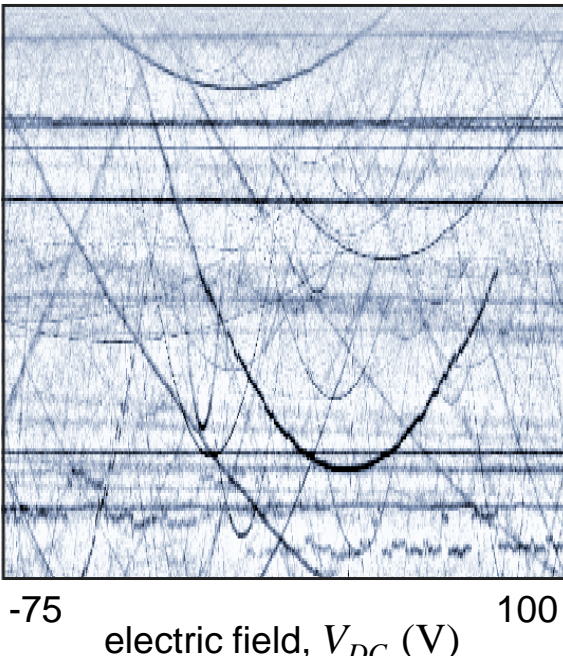
■ tune TLS resonance frequency



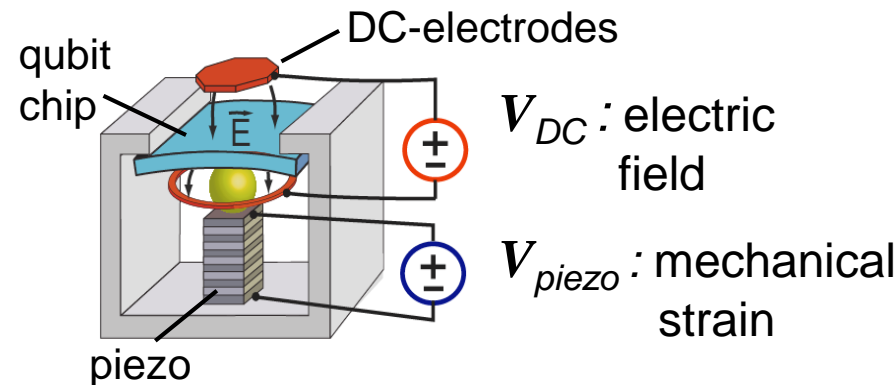
■ strain dependence



■ electric field dependence

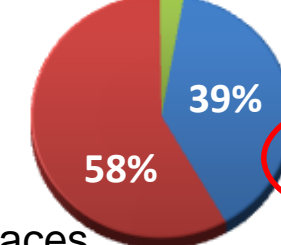


■ strain- and electric-field tuning



→ TLS locations:

in small junctions: 3%



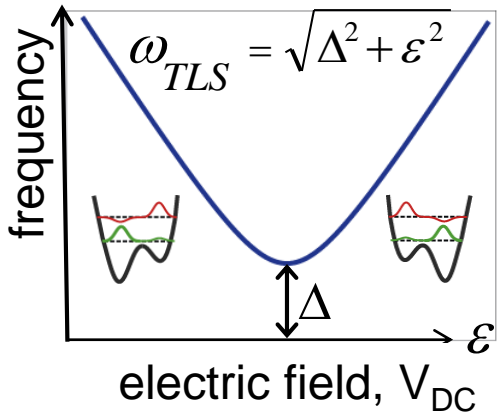
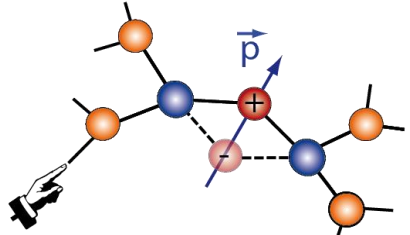
in stray JJs

on surfaces

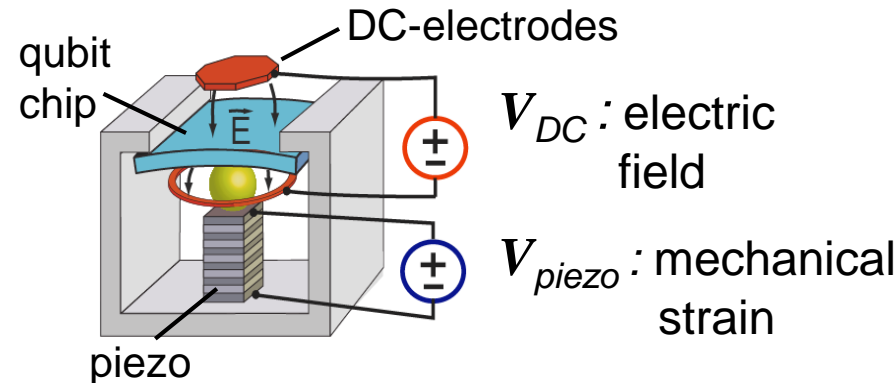
avoidable!

Controlling defects by Electric Fields

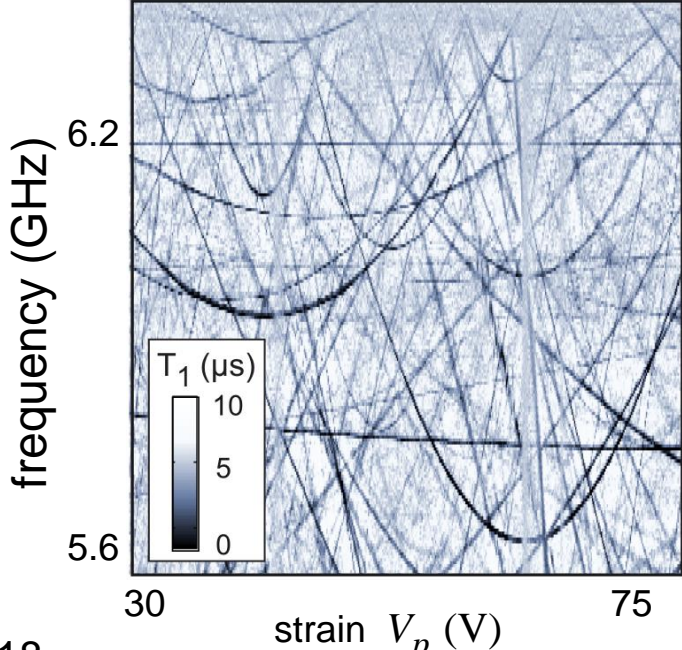
■ tune TLS resonance frequency



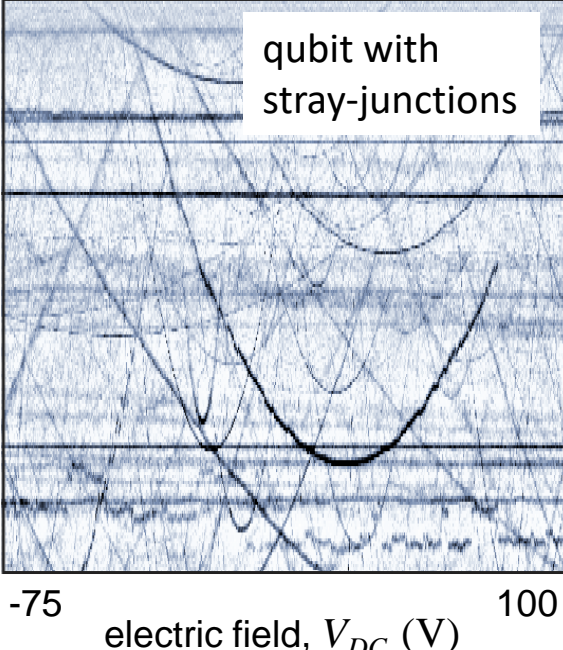
■ strain- and electric-field tuning



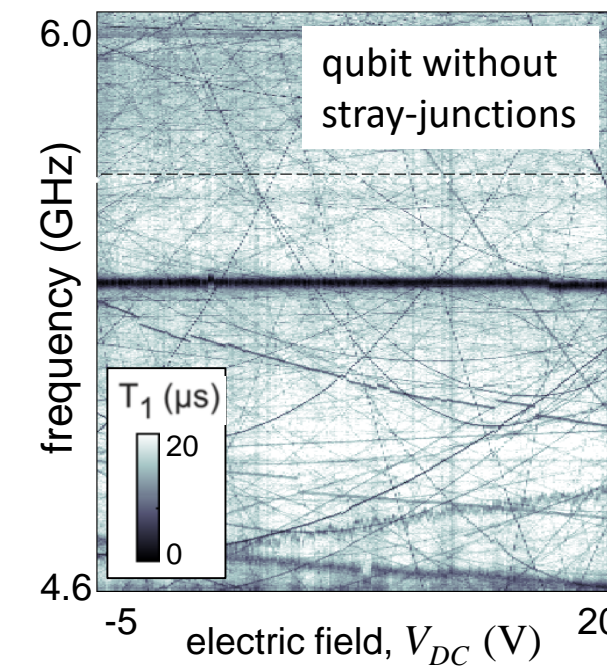
■ strain dependence



■ electric field dependence



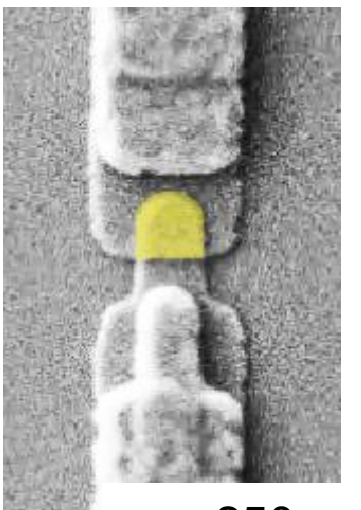
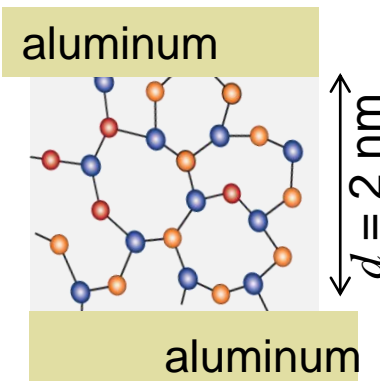
A. Bilmes, JL et al., *Supercond. Sci. Tech.* **34**, 125011 (2021)



Typical number of Junction-TLS:
~ 0.1 TLS / GHz
(200nm x 250nm JJ)

Decoherence due to junction-TLS

- TLS in the tunnel barrier



↔ 250nm
A. Bilmes, KIT

- qubit decay rate
due to a single junction-TLS:

$$\Gamma_1 \approx g^2 \frac{\Gamma_{TLS}}{\Gamma_{TLS}^2 + \delta^2}$$

→ $\Gamma_1 \approx (125 \mu\text{s})^{-1}$
for 2 TLS at detuning $\delta \pm 5 \text{ GHz}$
and 2 junctions in parallel at typical TLS densities

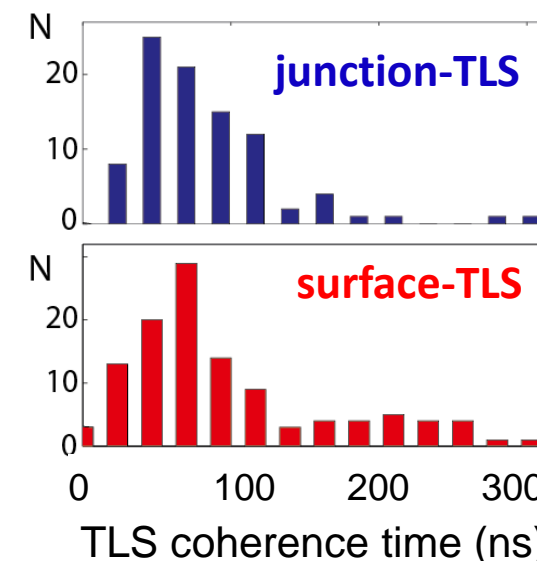
- $g = \left(\frac{\Delta_0}{E} \right) \vec{p} \cdot \vec{E} \approx 50 \text{ MHz}$
TLS-qubit coupling strength

E-field in tunnel barrier:

$$|\vec{E}| = \sqrt{\frac{\hbar\omega}{2C}} \frac{1}{d} \approx 2 \text{ kV/m}$$

TLS dipole moment $\vec{p} \approx 1e\text{\AA}$

- $\Gamma_{TLS} \approx 10 \text{ MHz}$
TLS decoherence rate

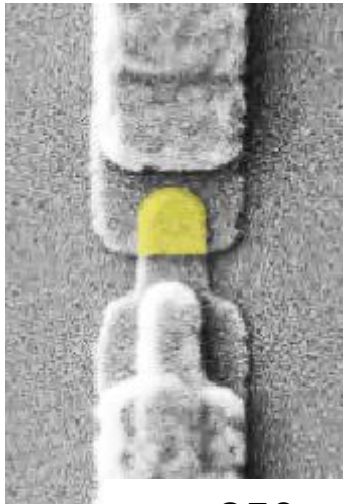
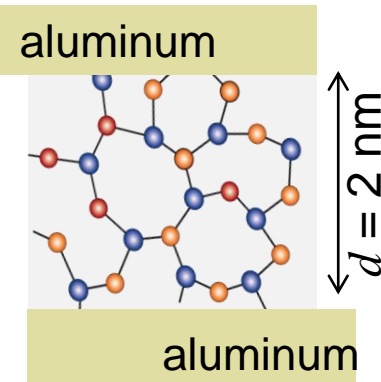


$$(\Gamma_1/2 + \Gamma_\phi)^{-1}$$

(Lisenfeld et al.,
npj quant. Inf. 5 (2019))

Decoherence due to junction-TLS

- TLS in the tunnel barrier



↔ 250nm
A. Bilmes, KIT

- qubit decay rate
due to a single junction-TLS:

$$\Gamma_1 \approx g^2 \frac{\Gamma_{TLS}}{\Gamma_{TLS}^2 + \delta^2}$$

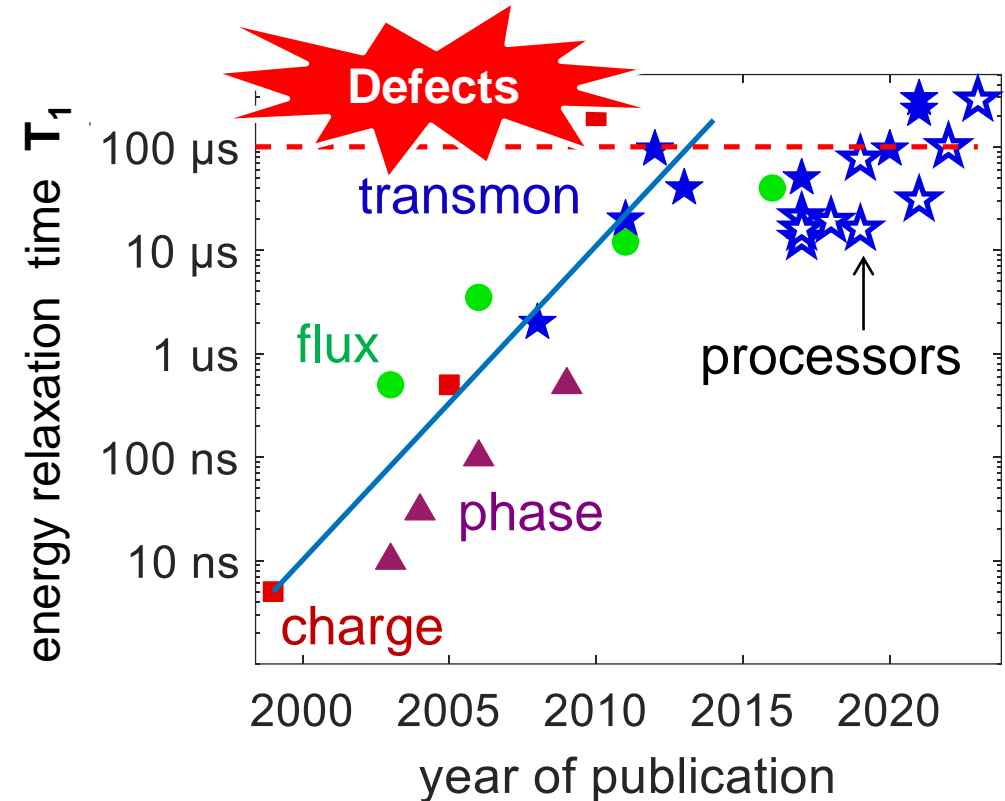
- $g = \left(\frac{\Delta_0}{E}\right) \vec{p} \cdot \vec{E} \approx 50 \text{ MHz}$
TLS-qubit coupling strength

E-field in tunnel barrier:

$$|\vec{E}| = \sqrt{\frac{\hbar\omega}{2C}} \frac{1}{d} \approx 2 \text{ kV/m}$$

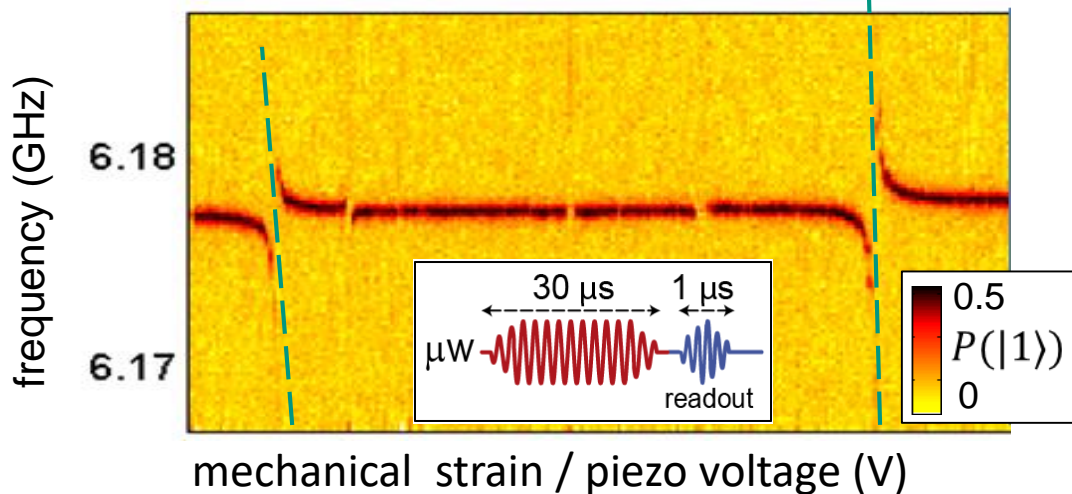
TLS dipole moment $\vec{p} \approx 1e\text{\AA}$

→ $\Gamma_1 \approx (125 \mu\text{s})^{-1}$
for 2 TLS at detuning $\delta \pm 5 \text{ GHz}$
and 2 junctions in parallel at typical TLS densities



qubit resonance with junction-TLS

avoided level crossings with TLS in JJs



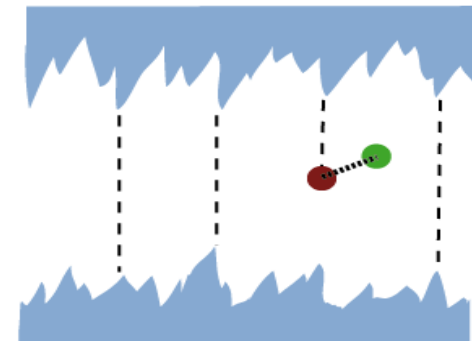
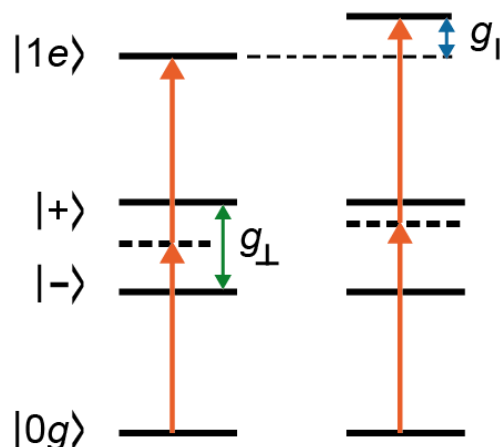
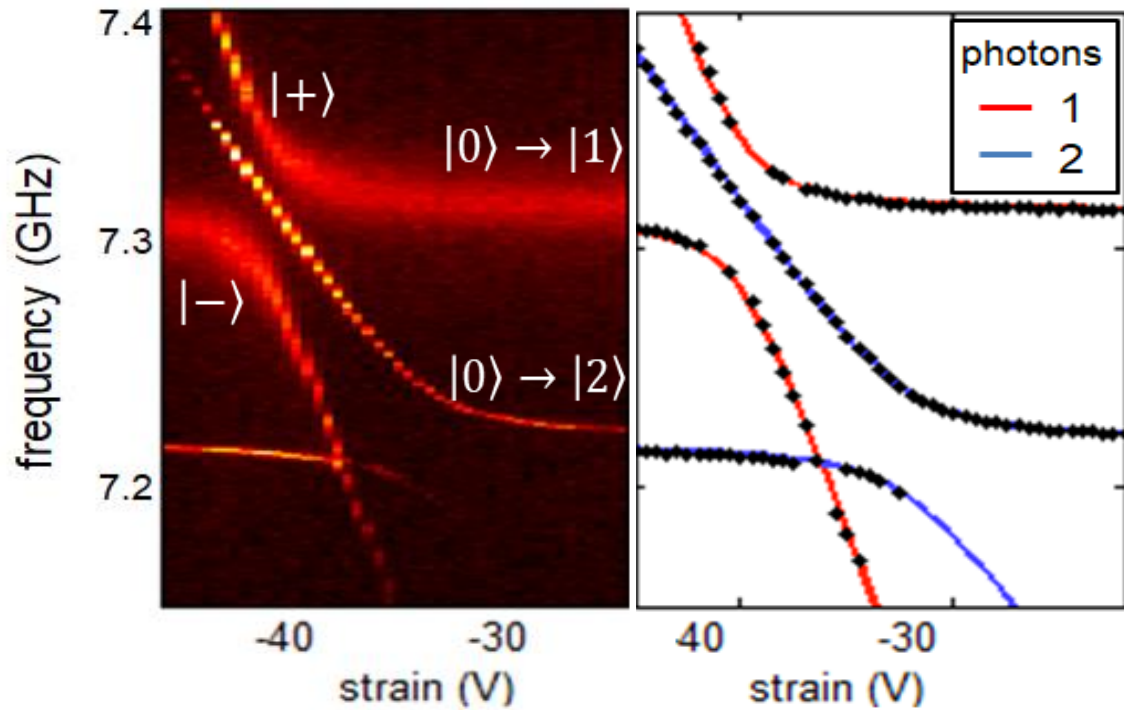
→ position of two-photon line reveals couplings between qubit and TLS

g_{\perp} : transversal / charge or

$g_{||}$: longitudinal / critical current

→ no detectable critical current coupling
 $g_{\perp} = 31.9 \text{ MHz}$, $g_{||} < 1 \text{ MHz}$

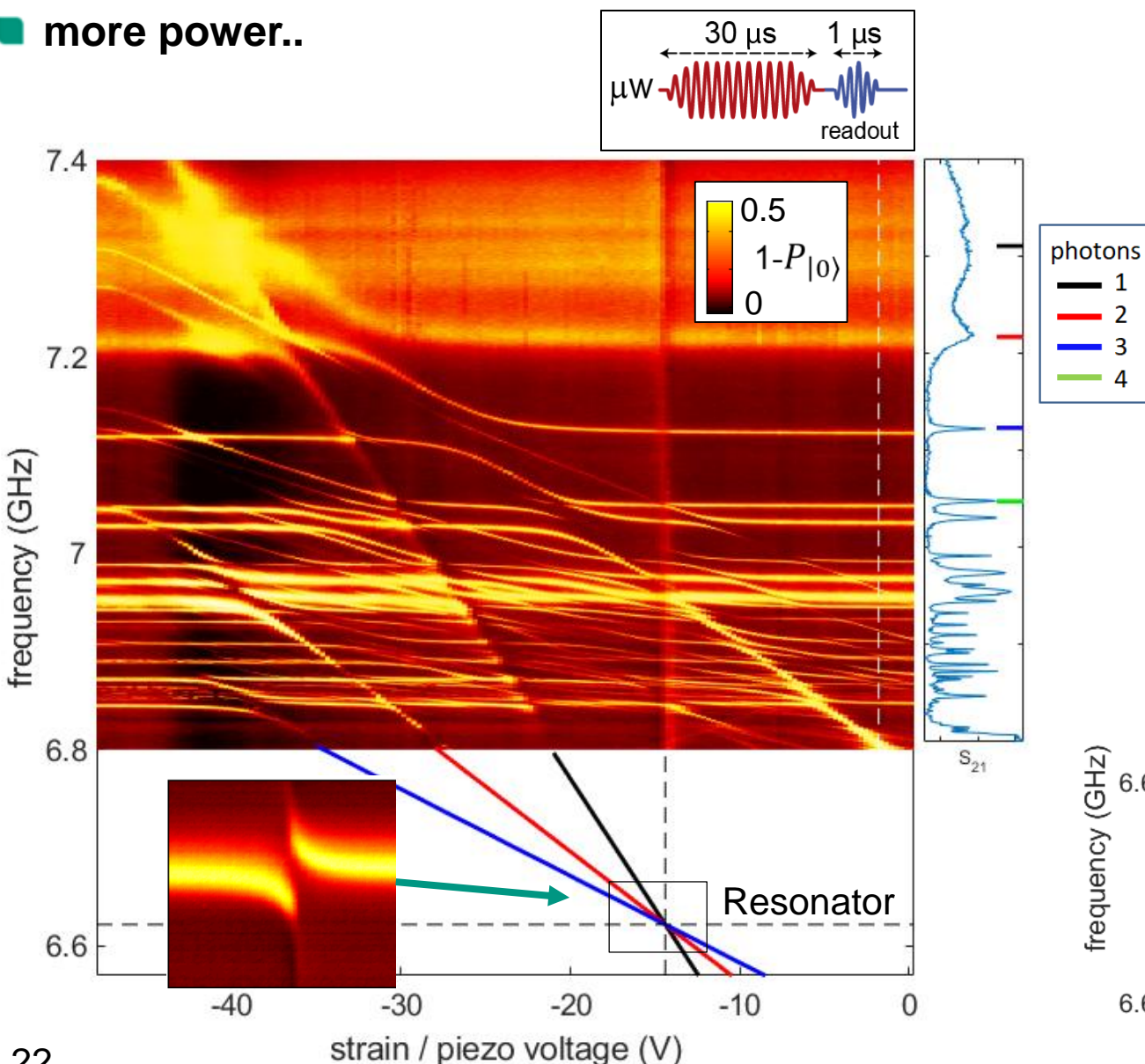
■ higher power: multi-photon transitions



TLS blocking tunneling channels in a JJ

Spectrum of TLS-Qubit-Resonator interactions

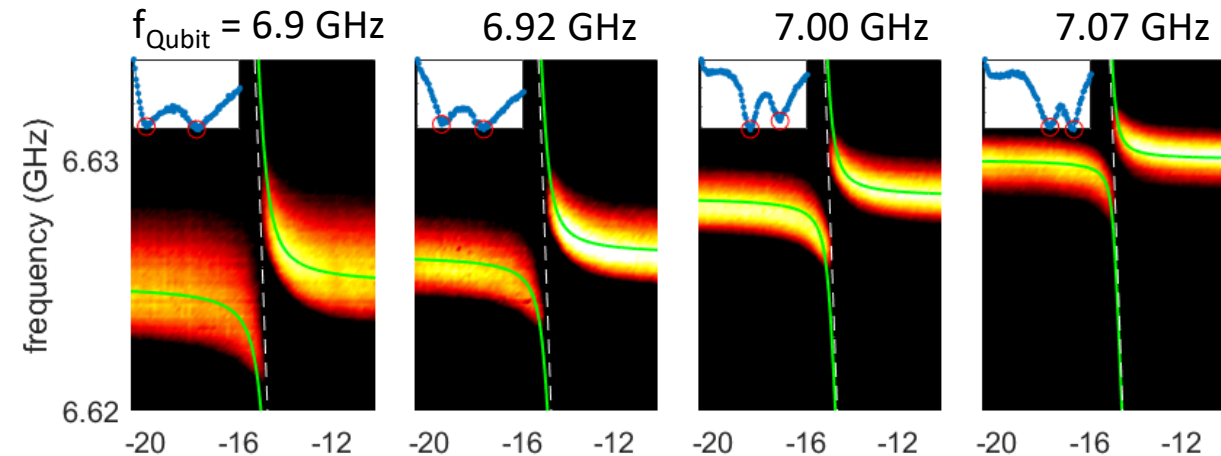
more power..



→ strong coupling of TLS to resonator mediated via qubit

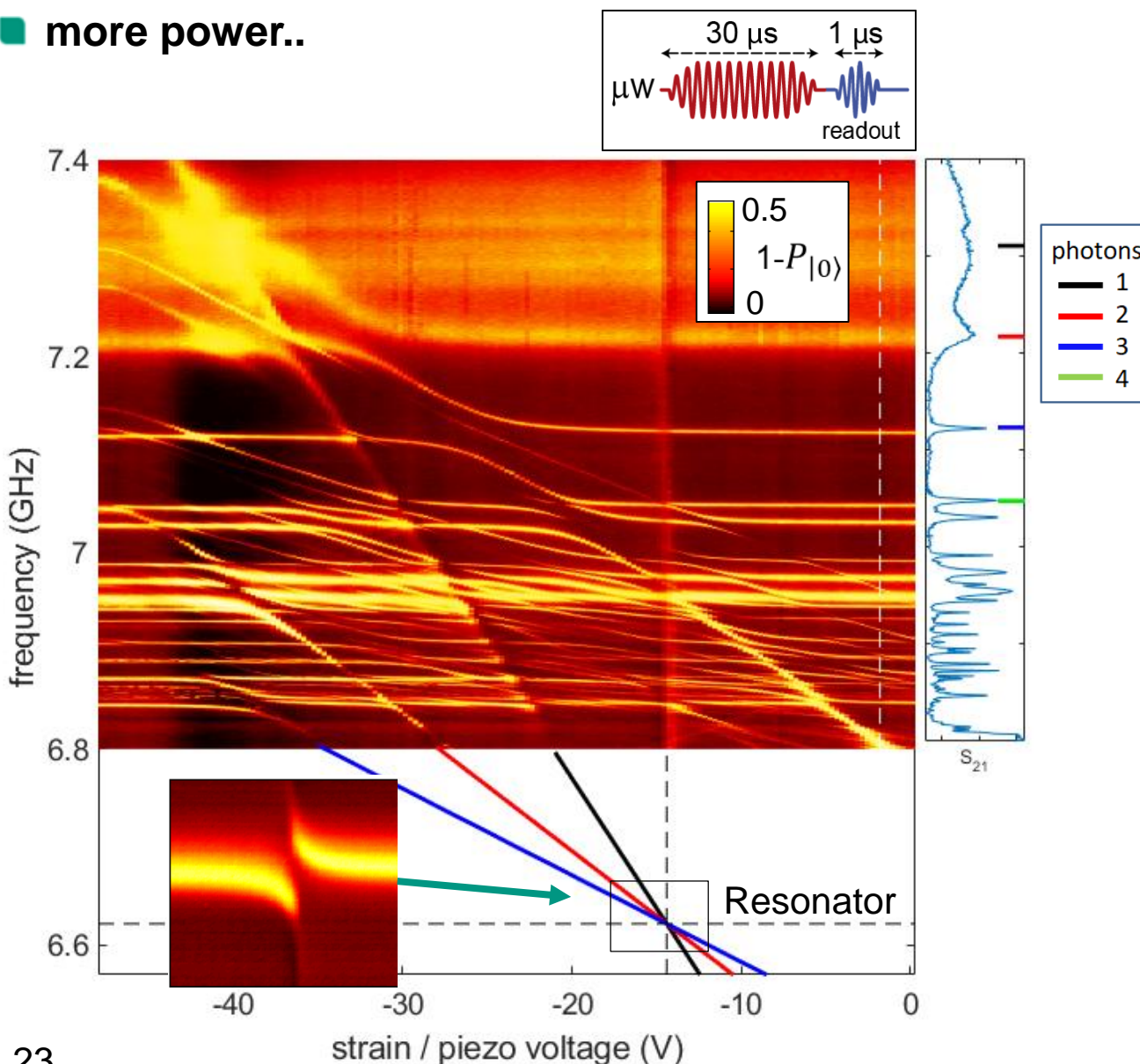
→ reveals new decoherence channel

TLS-resonator coupling strength vs. qubit detuning

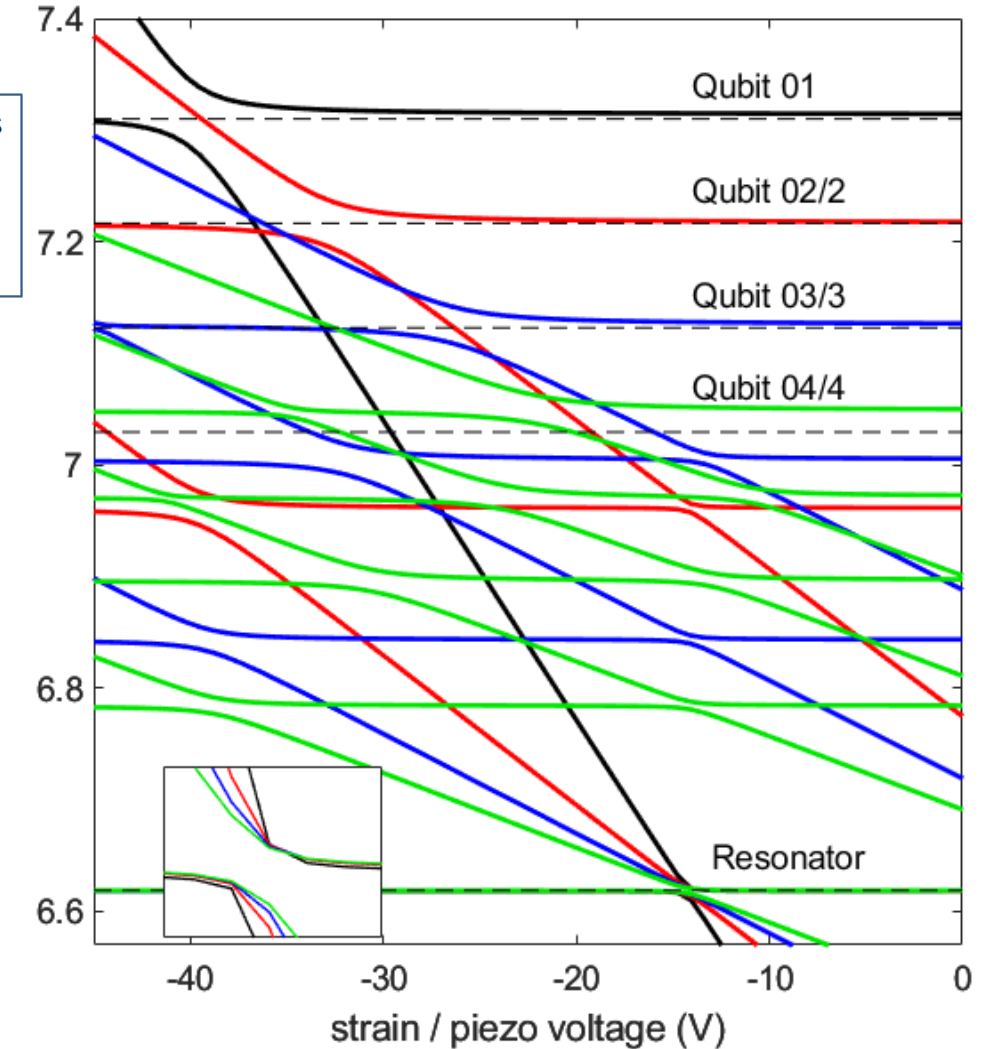


Spectrum of TLS-Qubit-Resonator interactions

more power..

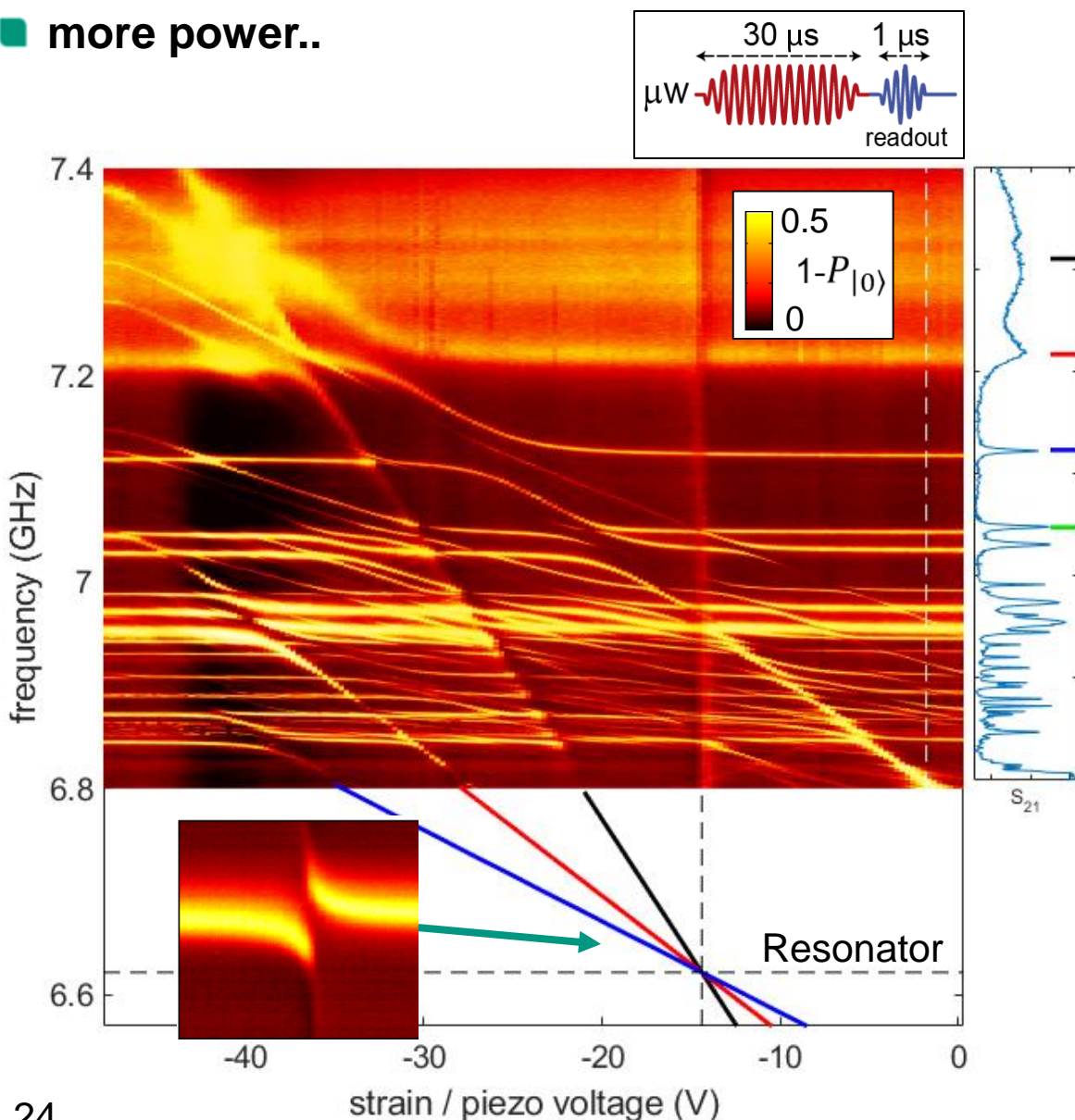


Eigenvalues of Hamiltonian



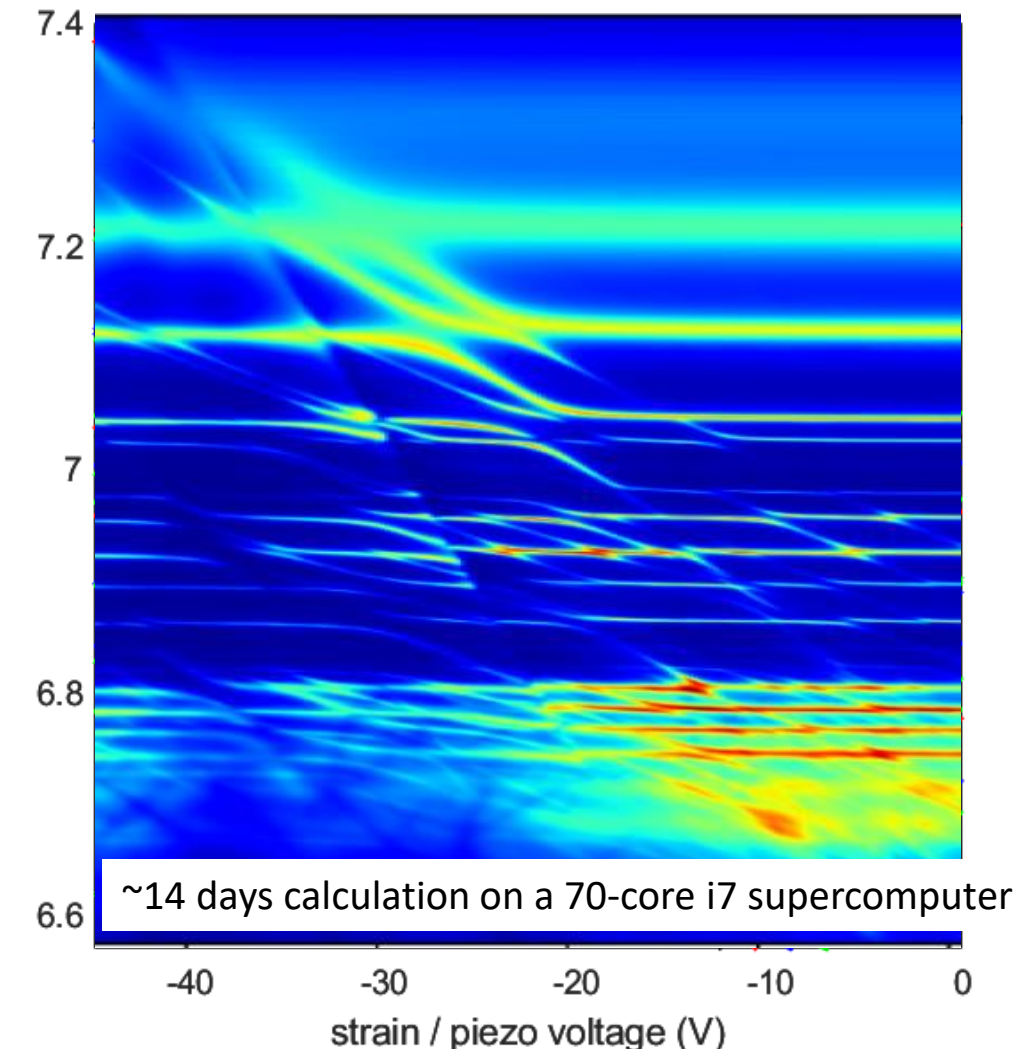
Spectrum of TLS-Qubit-Resonator interactions

more power..



simulation of driven system (Qutip)

qubit expectation value



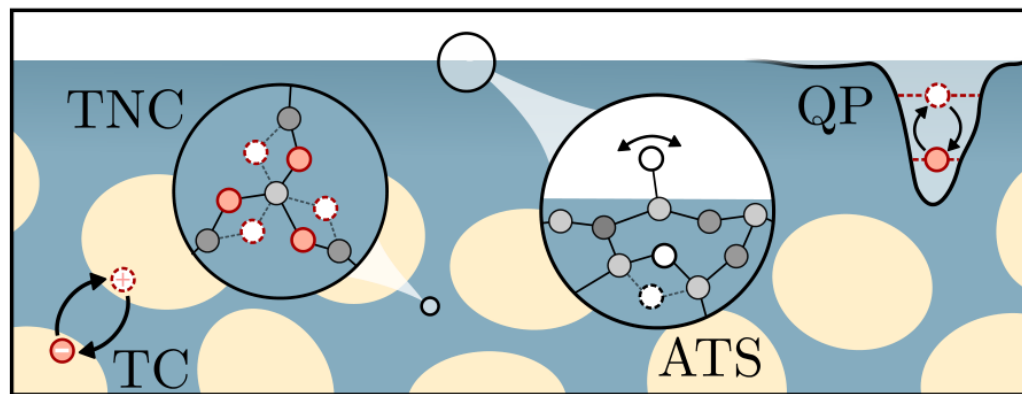
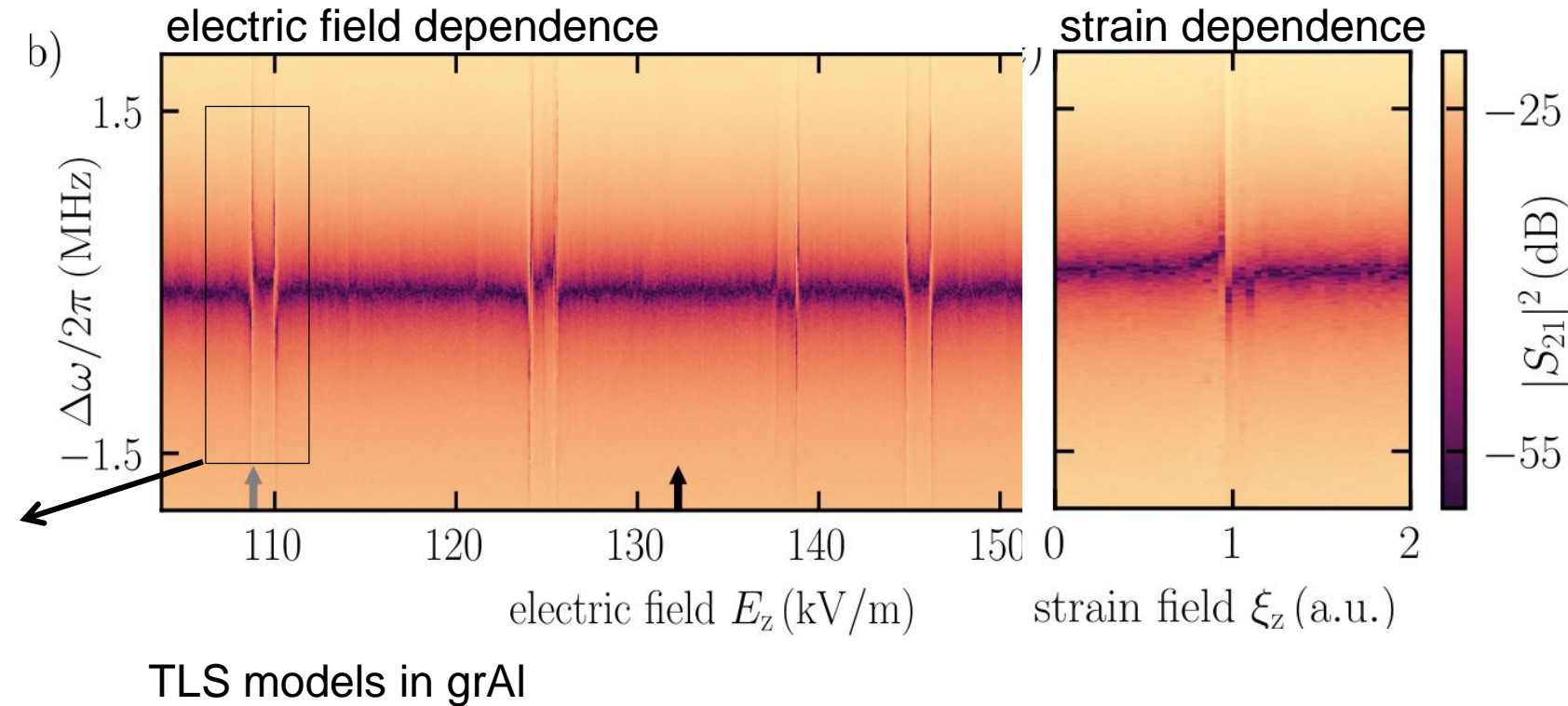
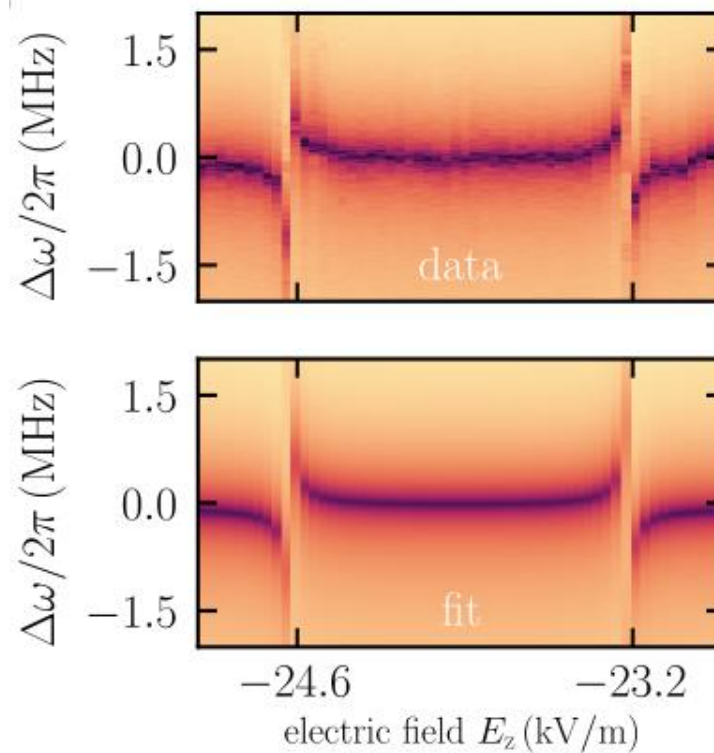
TLS in granular aluminum resonators

M. Kristen, N. Voss, M. Wildermuth, J. Lisenfeld,
H.R. Rotzinger and A.V. Ustinov, in prep. (2023)

stripline resonator:

- ~25 nm-thick grAl on Sapphire
- width = 2 μm , length=505 μm
- R_n : 0.68 $\text{k}\Omega/\square$
- resonance at 7.48 GHz

avoided level crossings



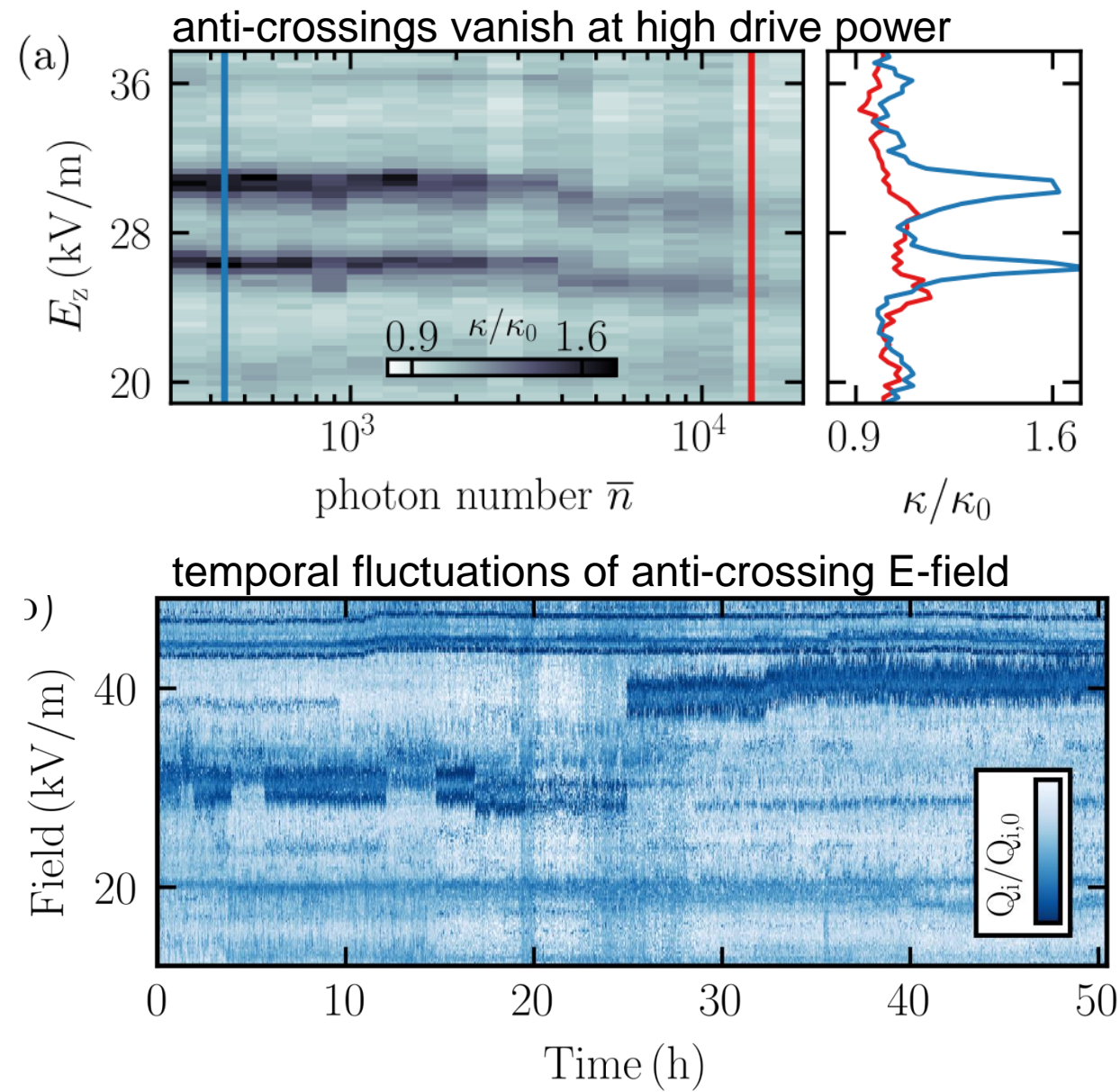
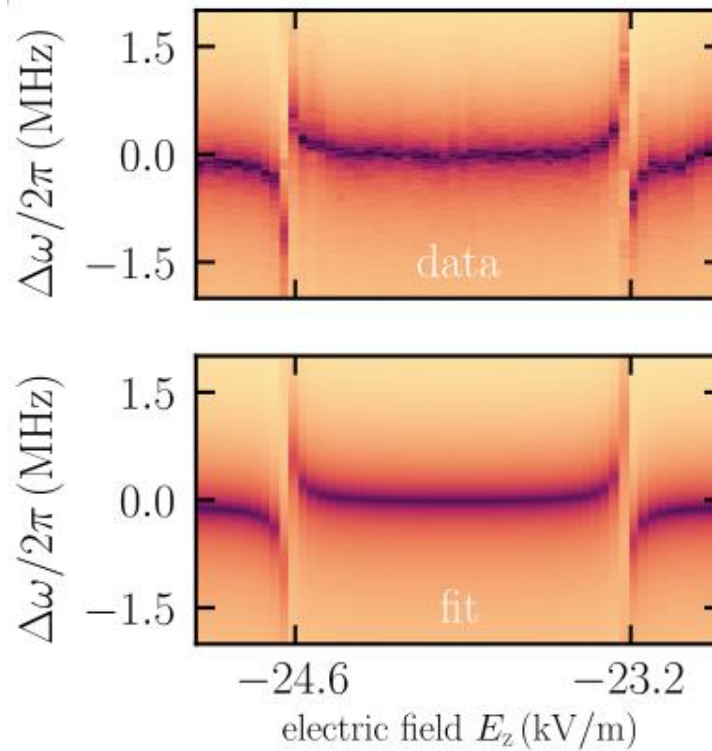
TLS in granular aluminum resonators

M. Kristen, N. Voss, M. Wildermuth, J. Lisenfeld,
H.R. Rotzinger and A.V. Ustinov, in prep. (2023)

stripline resonator:

- ~25 nm-thick grAl on Sapphire
- width = 2 nm, length=505 nm
- R_n : 0.68 k Ω/\square
- resonance at 7.48 GHz

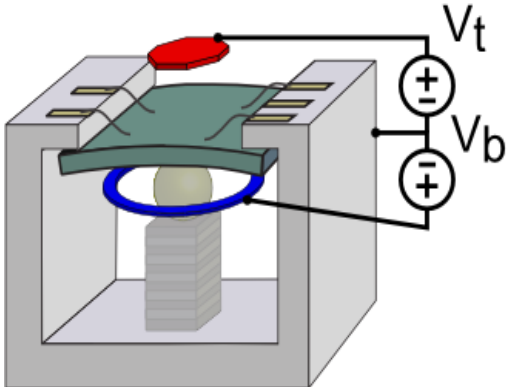
avoided level crossings



determine locations of surface-TLS

A. Bilmes, A. Megrant, P. Klimov, G. Weiss, J.M. Martinis, A.V. Ustinov,
and J. Lisenfeld., Scientific Reports 10, 3090 (2020)

■ two independent DC-electrodes

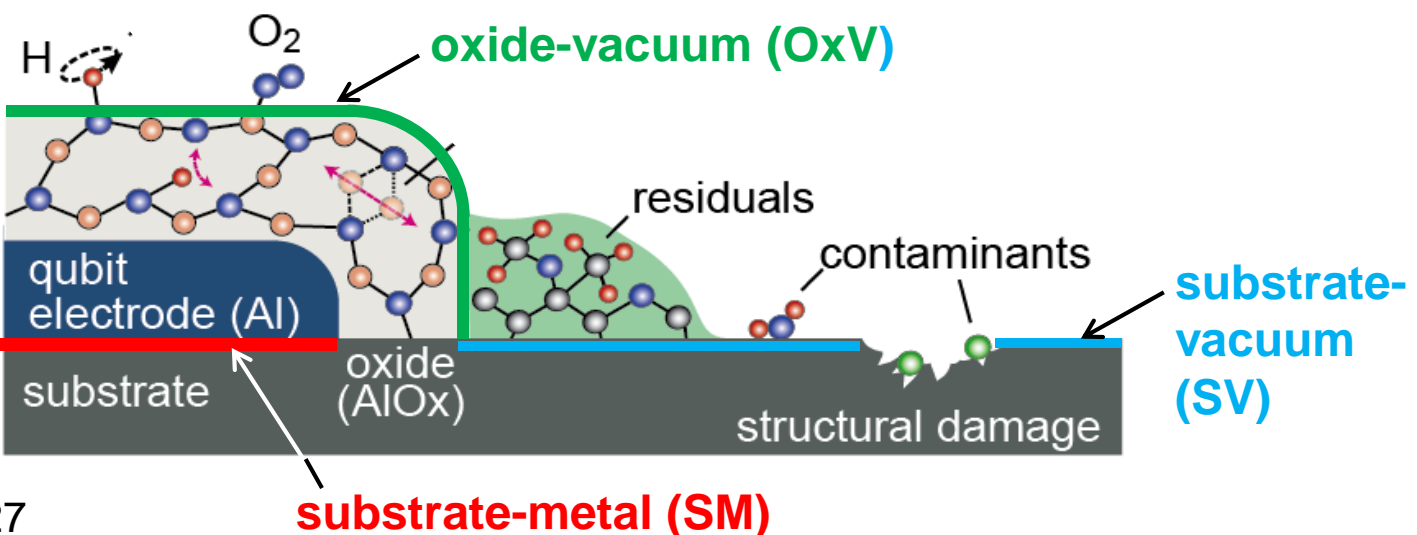


measure simulate

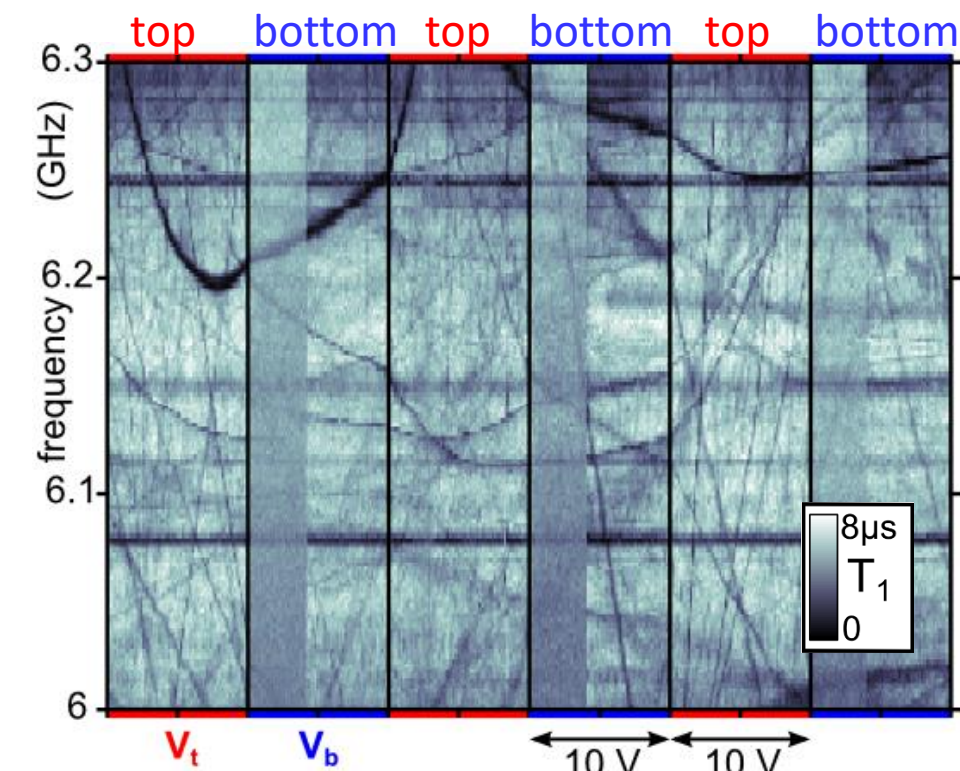
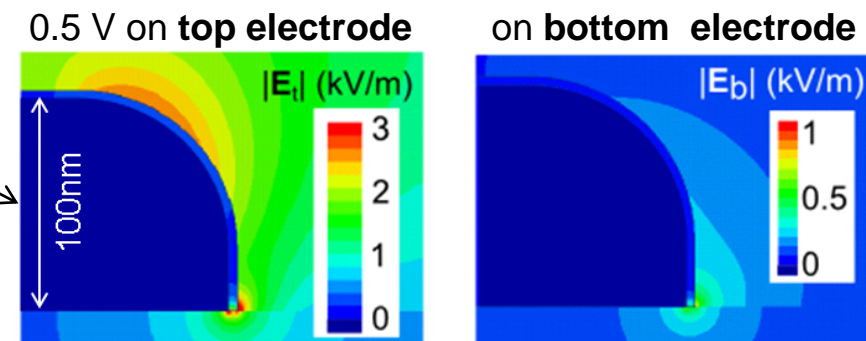
$$\frac{\gamma_t}{\gamma_b} \frac{V_t}{V_b} = \frac{dE_t(x)}{dE_b(x)}$$

then solve for location x

distinguish TLS at different circuit interfaces



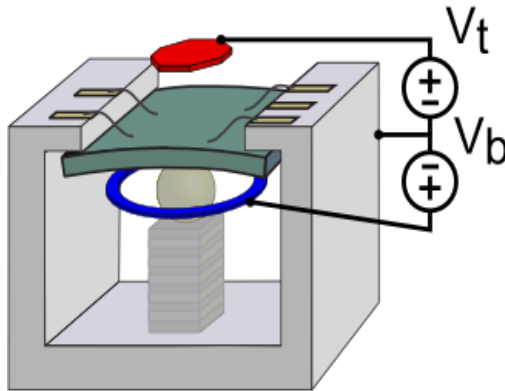
E-field simulations



determine locations of surface-TLS

A. Bilmes, A. Megrant, P. Klimov, G. Weiss, J.M. Martinis, A.V. Ustinov,
and J. Lisenfeld., Scientific Reports 10, 3090 (2020)

■ two independent DC-electrodes



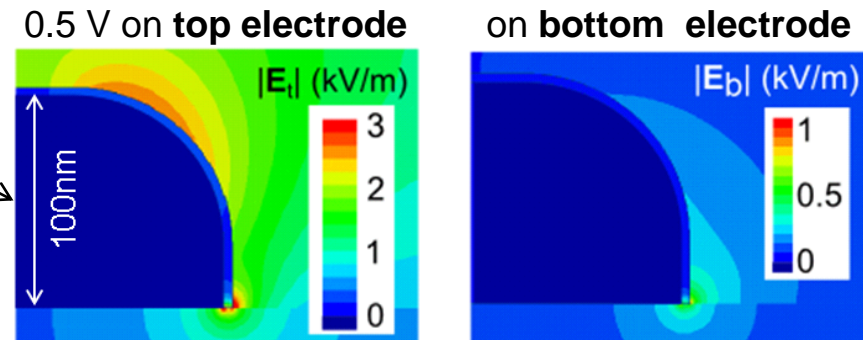
measure simulate

$$\frac{\gamma_t}{\gamma_b} \frac{V_t}{V_b} = \frac{dE_t(x)}{dE_b(x)}$$

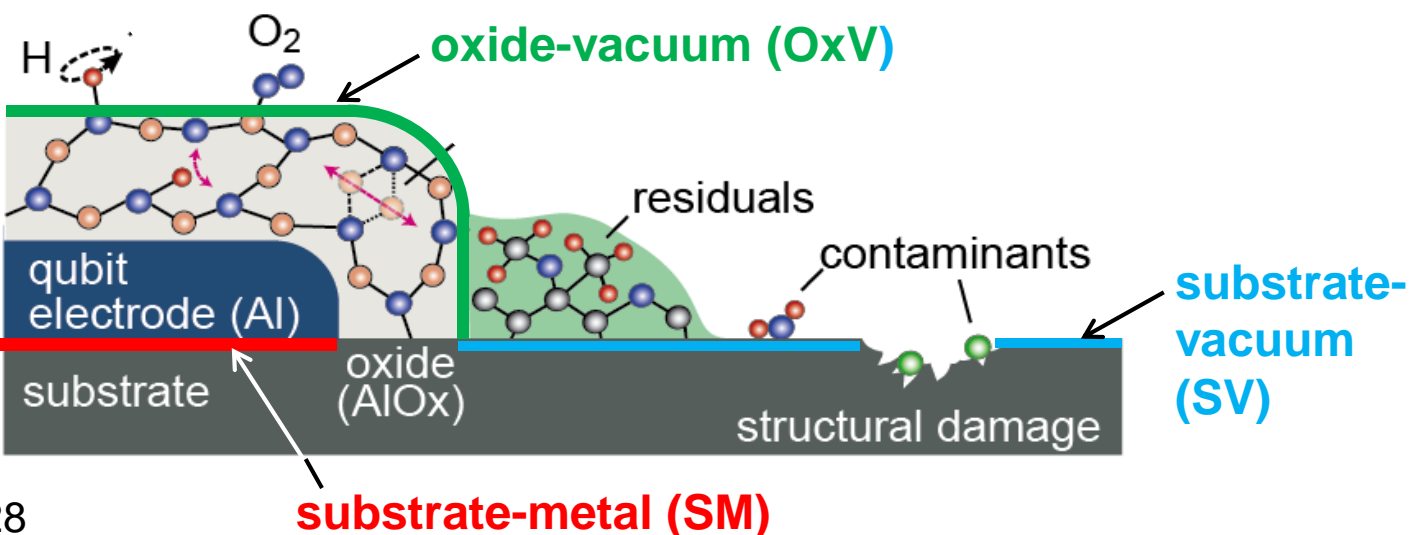
then solve for location x

qubit
electrode

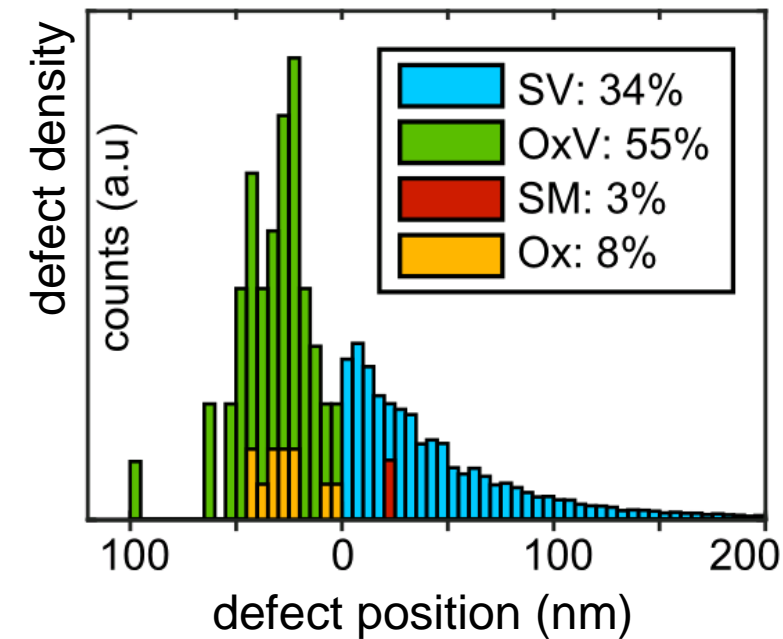
E-field simulations



distinguish TLS at different circuit interfaces

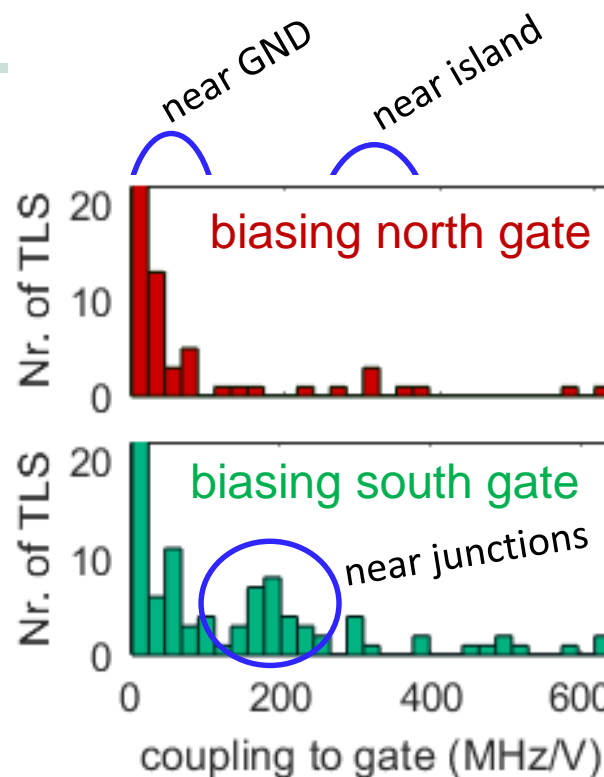
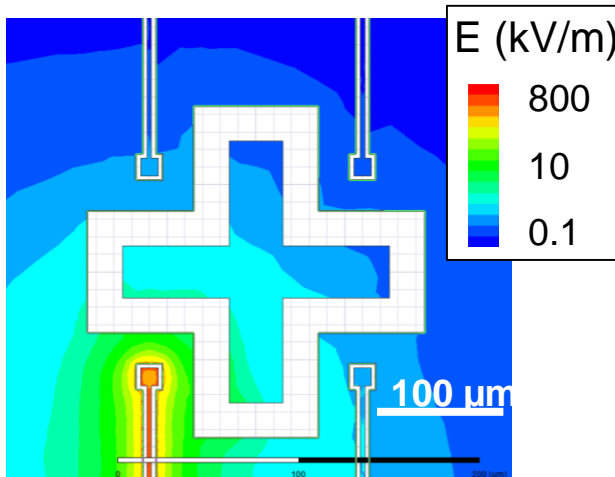
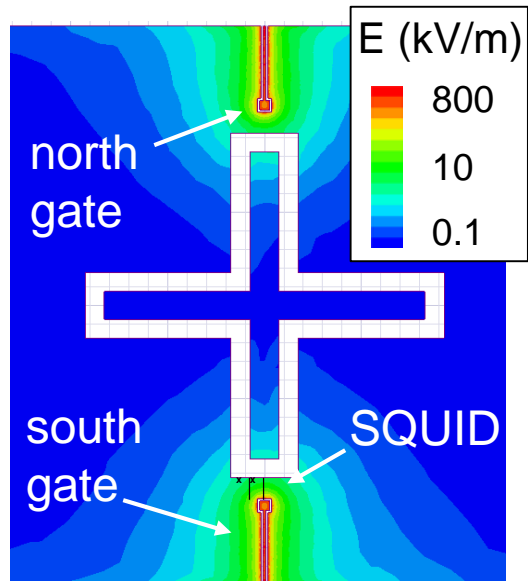


■ locations of TLS along film edge

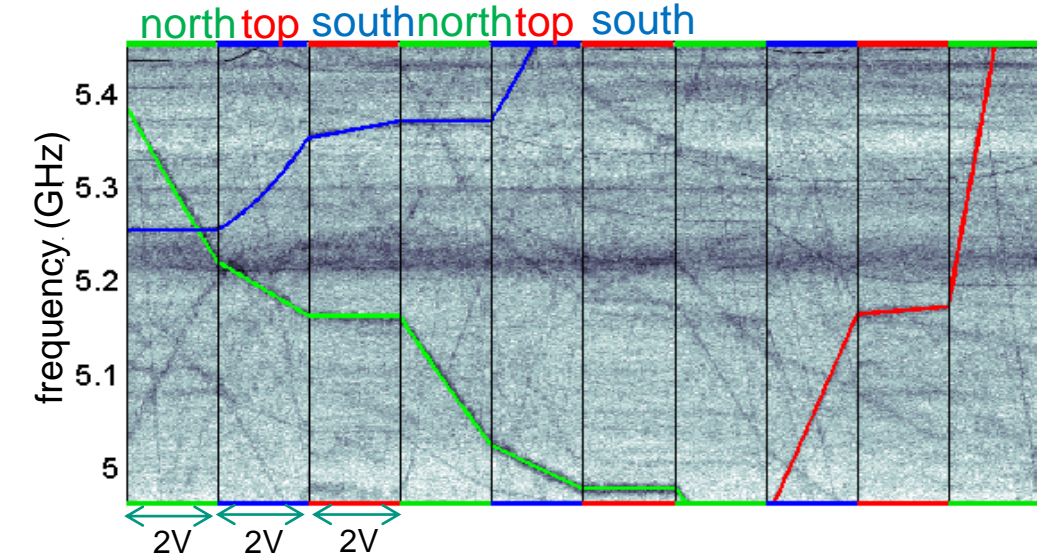


mapping TLS locations

on-chip gate electrodes



measure response of TLS to each electrode

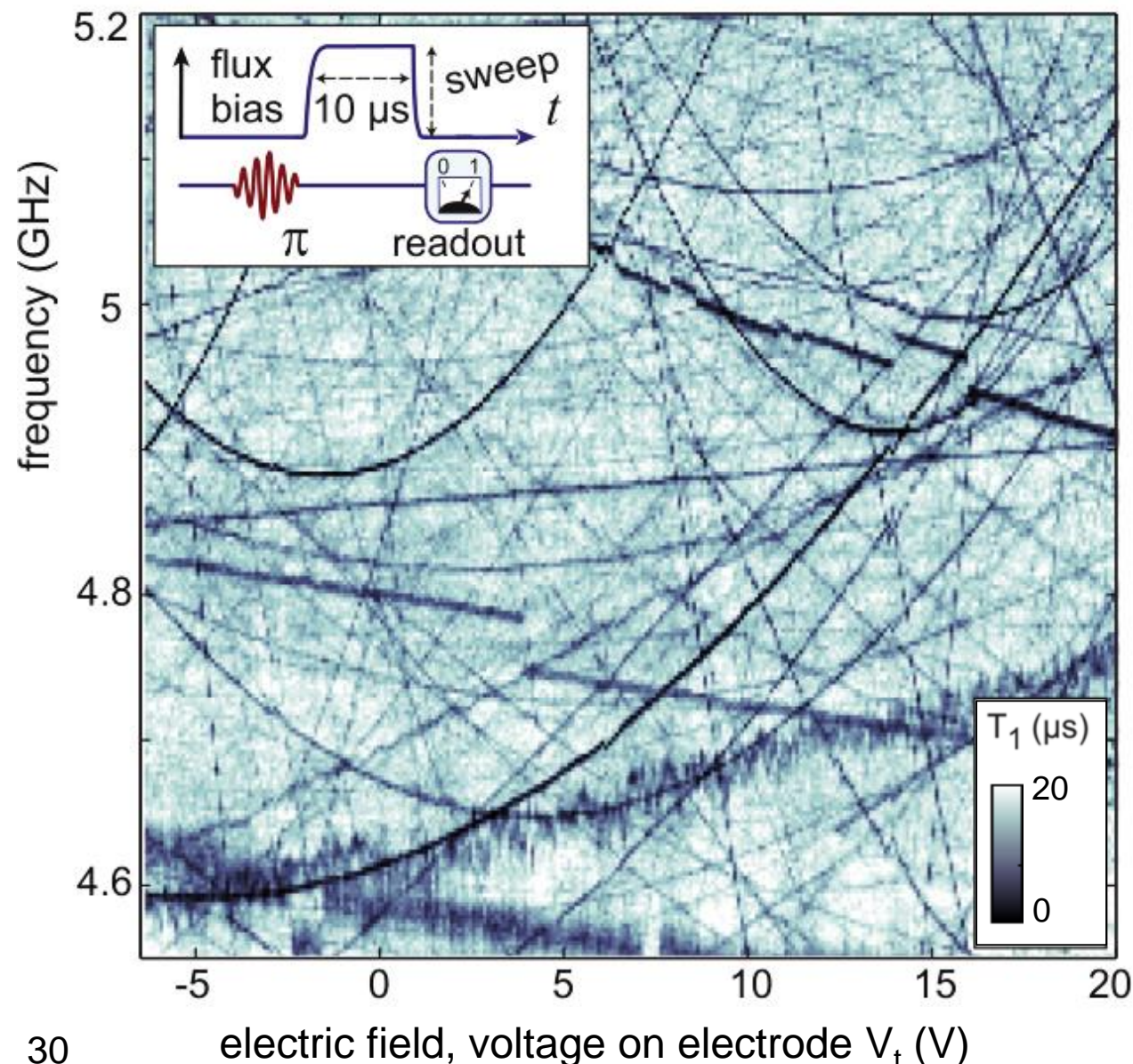


Goals:

- obtain 2D-maps of defect positions
- clarify role of TLS on junction leads
- compare TLS formation by optical and eBeam lithography, Ion-milling, residuals

Enhancing the T_1 -time of qubits by E-fields

J. Lisenfeld, A. Bilmes et al.,
npj Quant. Inf. 9, 8 (2023)



- Idea:

increase T_1 – time by tuning defects away from qubit resonance

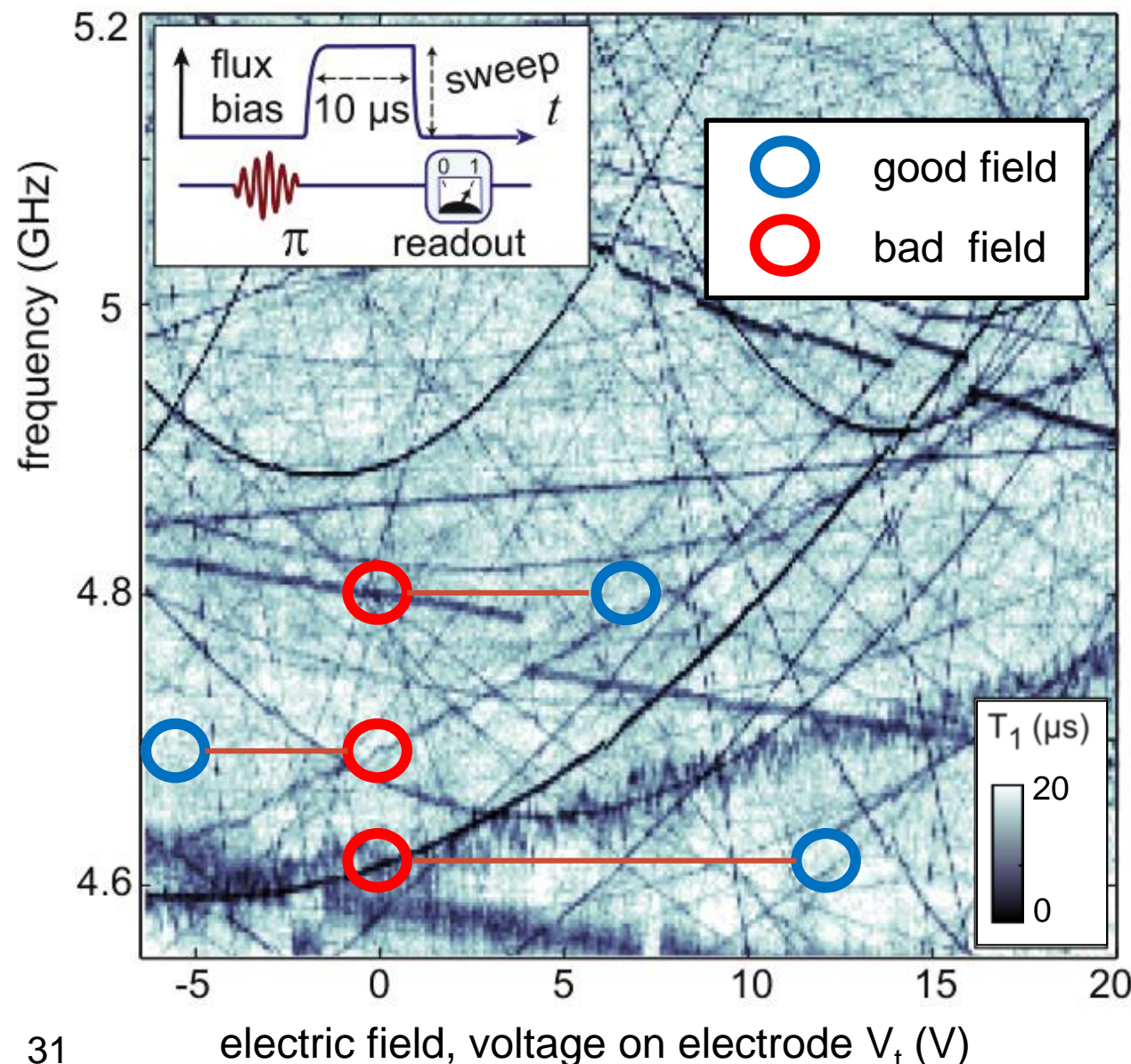
- Demo:

Enhancing the Coherence of Superconducting Qubits with Electric Fields

J. Lisenfeld, A. Bilmes, and A.V. Ustinov,
npj Quant. Inf. 9, 8 (2023)

Enhancing the T_1 -time of qubits by E-fields

J. Lisenfeld, A. Bilmes et al.,
npj Quant. Inf. 9, 8 (2023)



- Idea:

increase T_1 – time by tuning defects away from qubit resonance

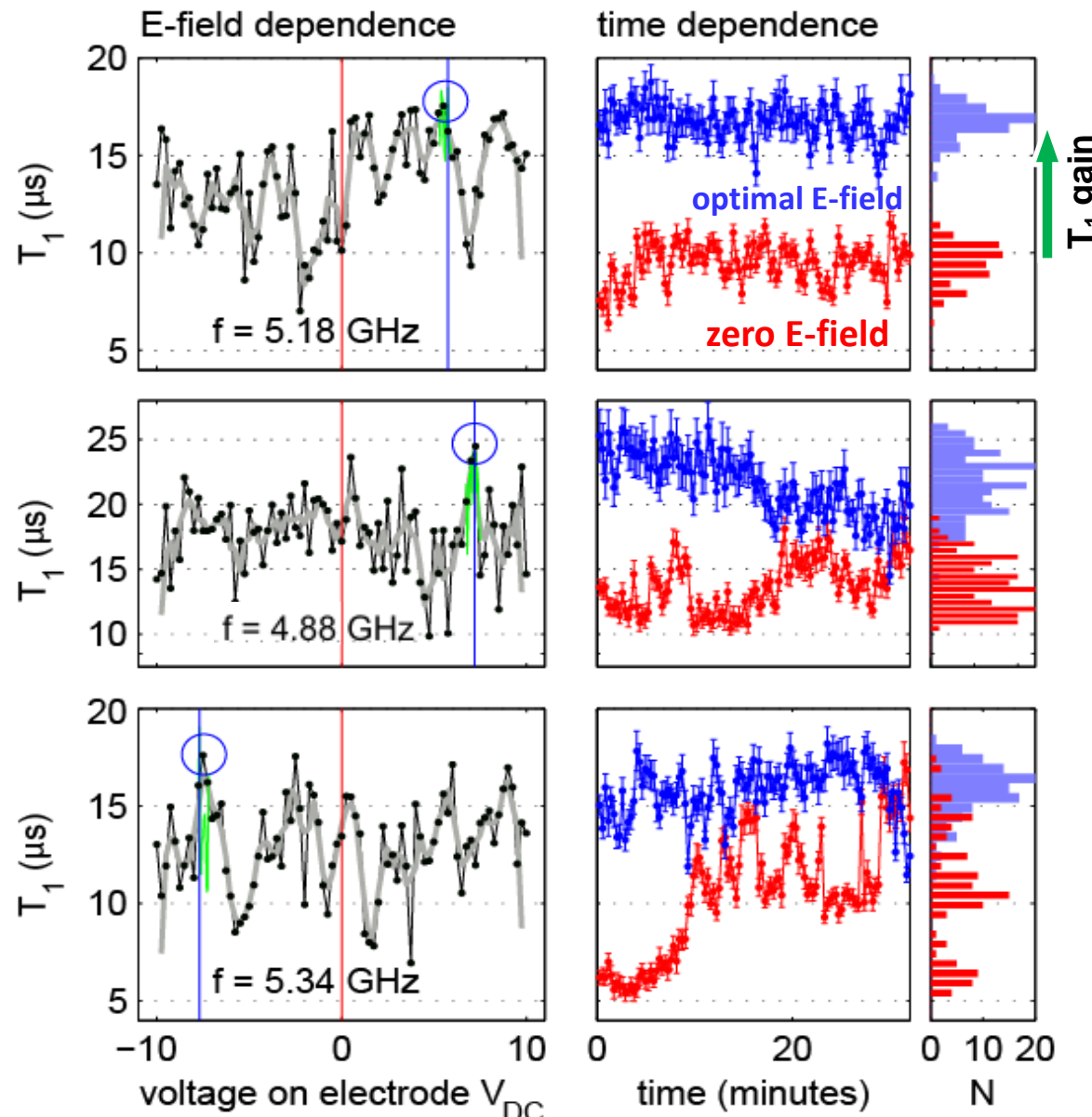
- Demo:

Enhancing the Coherence of Superconducting Qubits with Electric Fields

J. Lisenfeld, A. Bilmes, and A.V. Ustinov,
npj Quant. Inf. 9, 8 (2023)

Enhancing the T_1 -time of qubits by E-fields

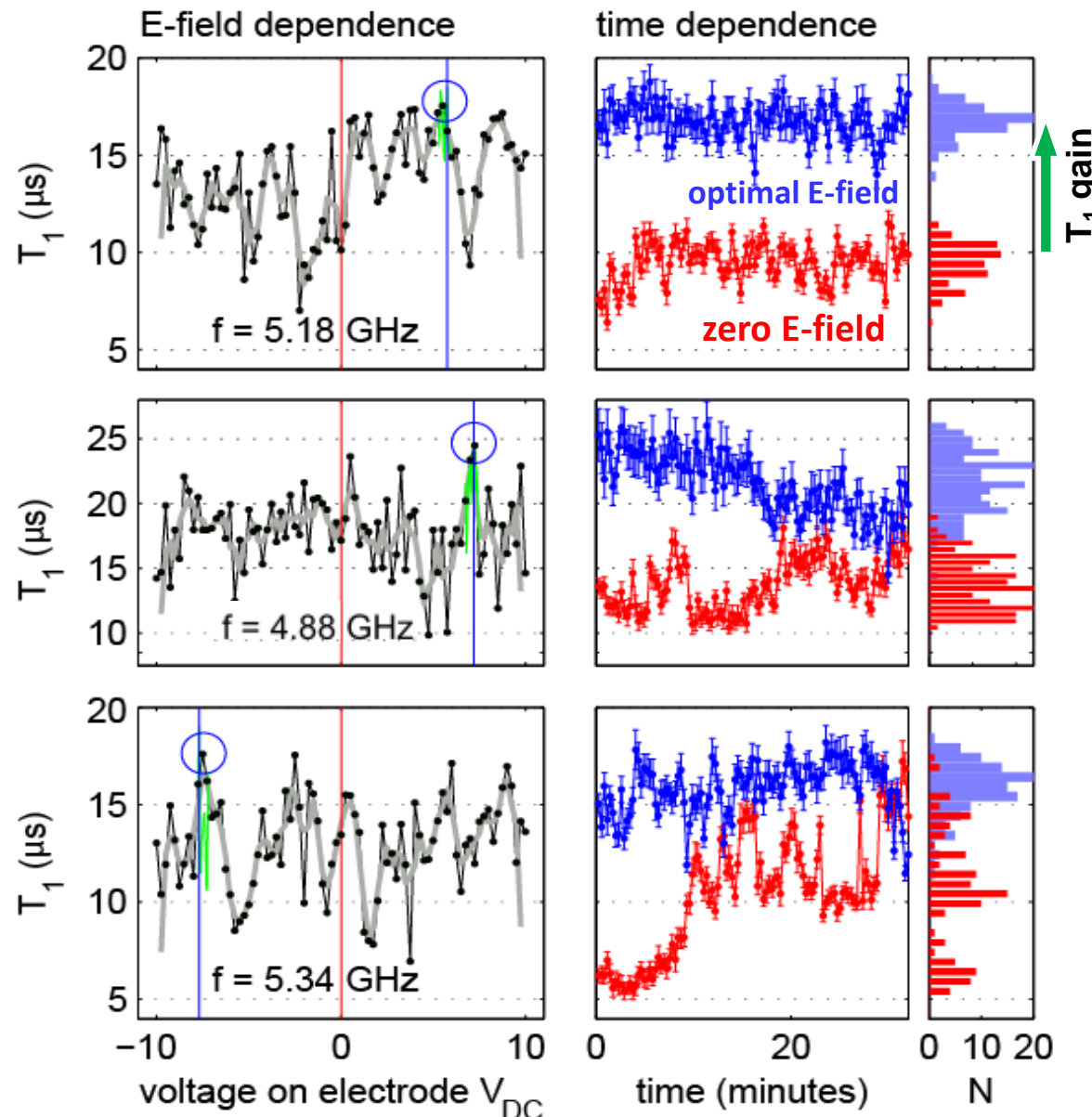
J. Lisenfeld, A. Bilmes et al.,
npj Quant. Inf. 9, 8 (2023)



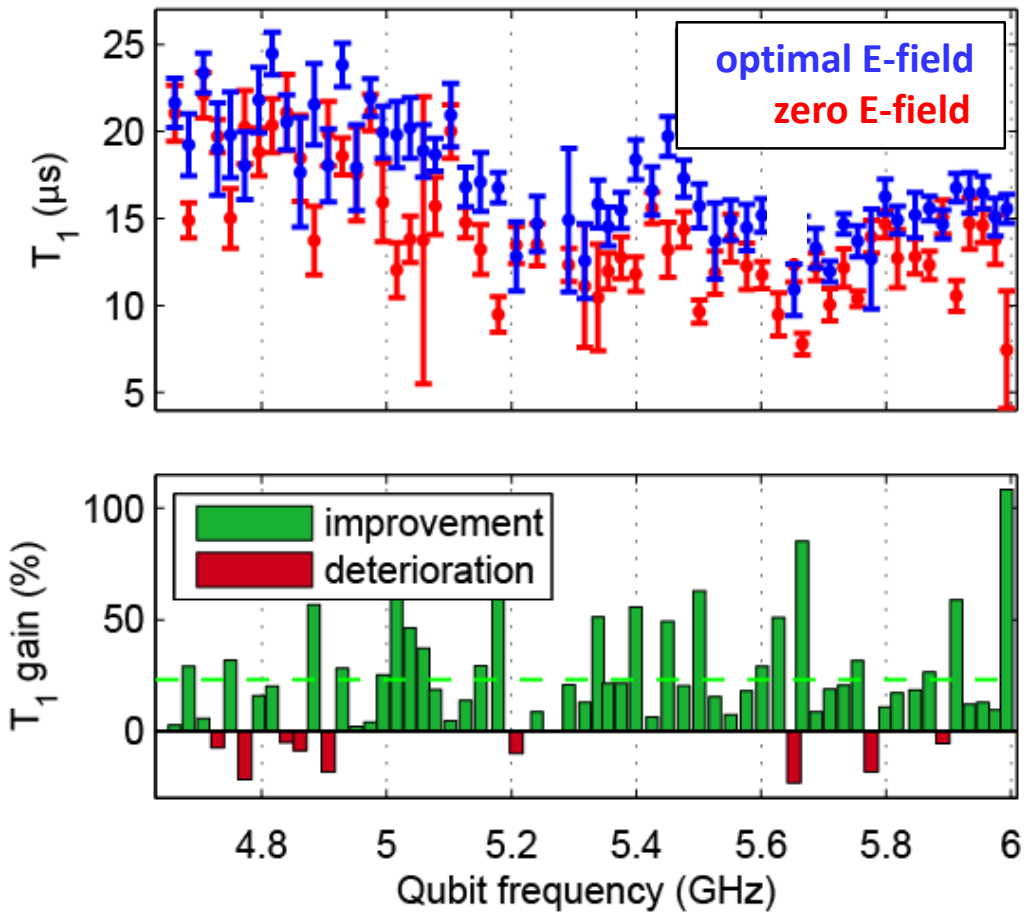
- **Method:**
Measure T_1 vs. applied E-field,
find optimal E-field where T_1 reaches maximum
- **Benchmark:**
Monitor T_1 for 30 minutes
at **zero** and **optimal** E-fields
repeat at various frequencies

Enhancing the T_1 -time of qubits by E-fields

J. Lisenfeld, A. Bilmes et al.,
npj Quant. Inf. 9, 8 (2023)



■ Results: automatically enhanced T_1 times

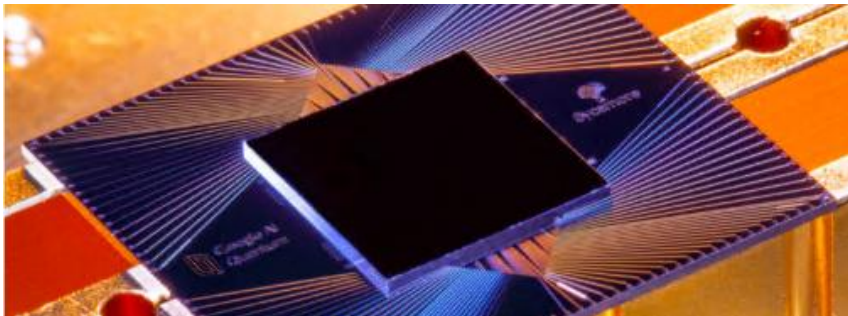


→ T_1 enhanced by ~ 23% on average

E-field tuning: Integration in quantum processors

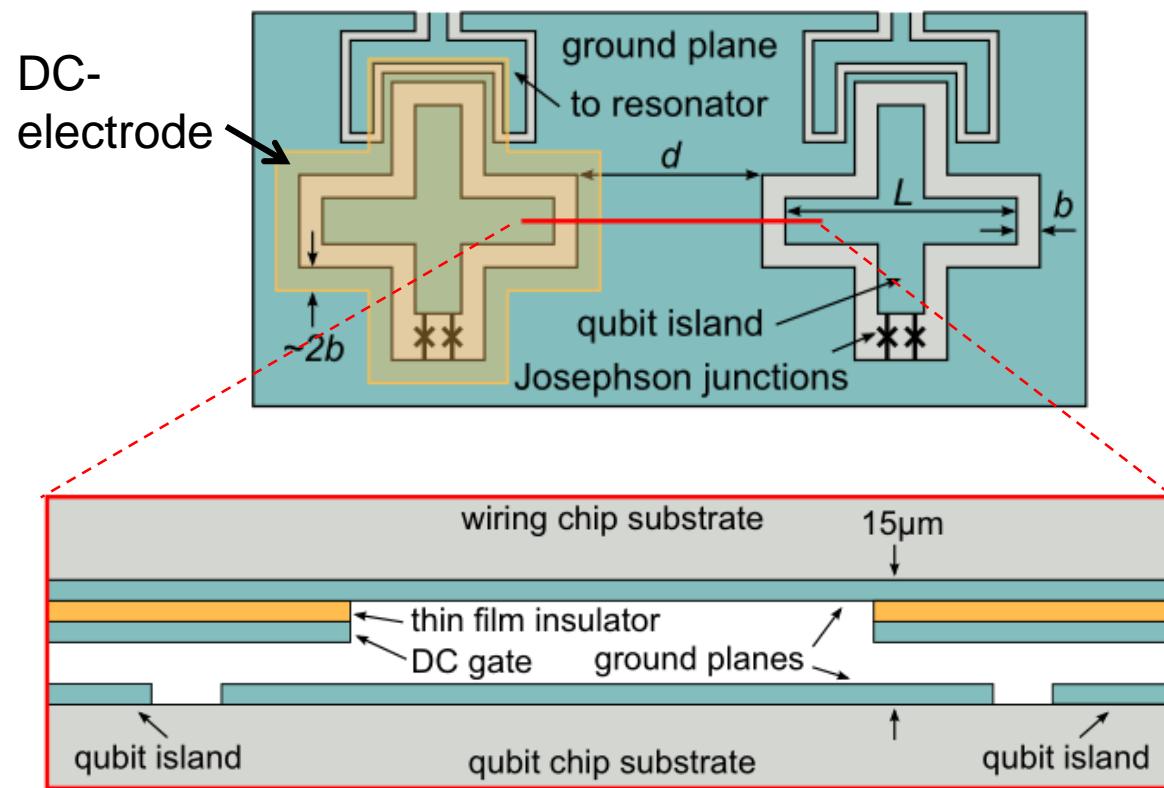
■ Flip-Chip architecture

- **Sycamore, 53-qubits, 86 tunable couplers** (Google)
F. Arute et al., nature 574, 505 (2019)



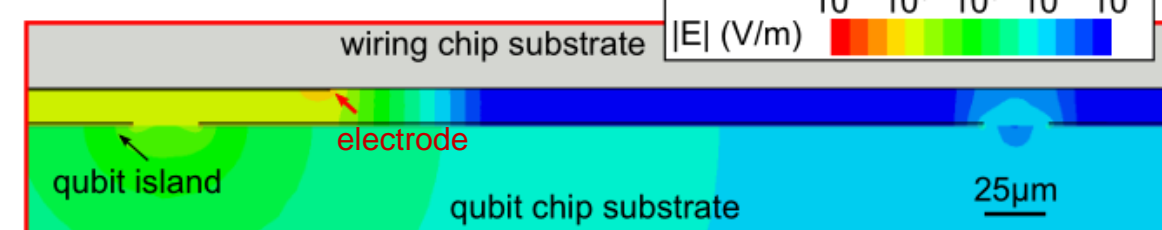
- easy to implement
- efficient (20+% more T_1 time)
- fast (<1 minute or on-the-fly)
- scalable to multi-qubit processors

■ Integration of DC-electrodes

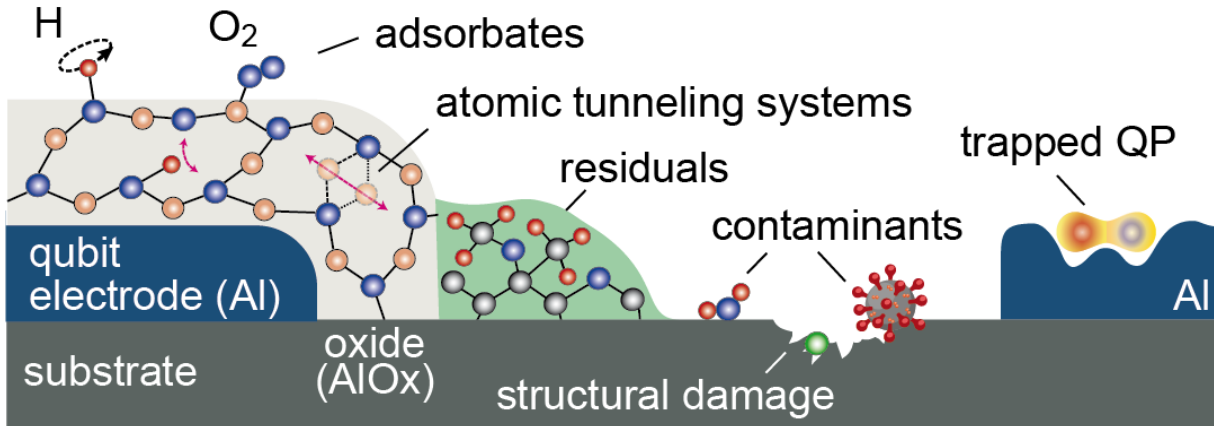


E-field simulation

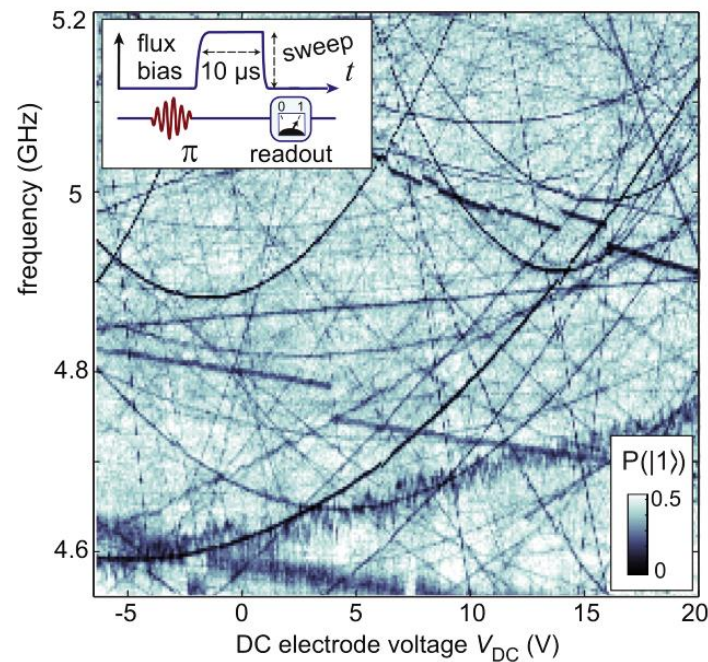
→ small crosstalk $\sim 10^{-4}$



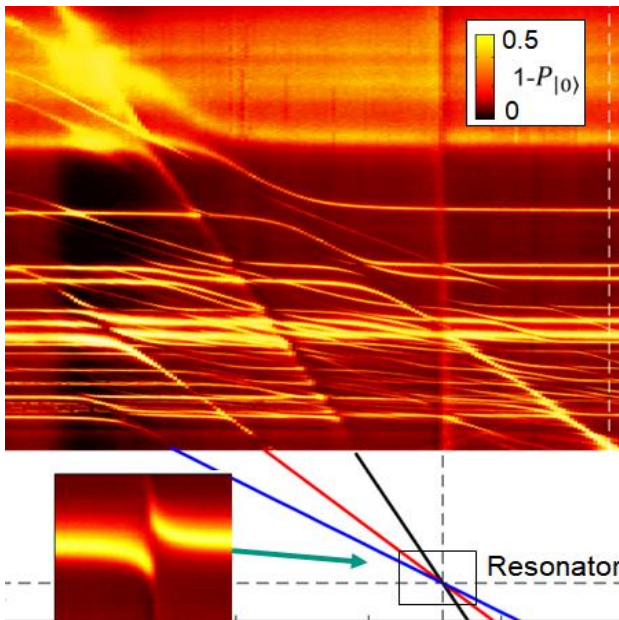
Summary



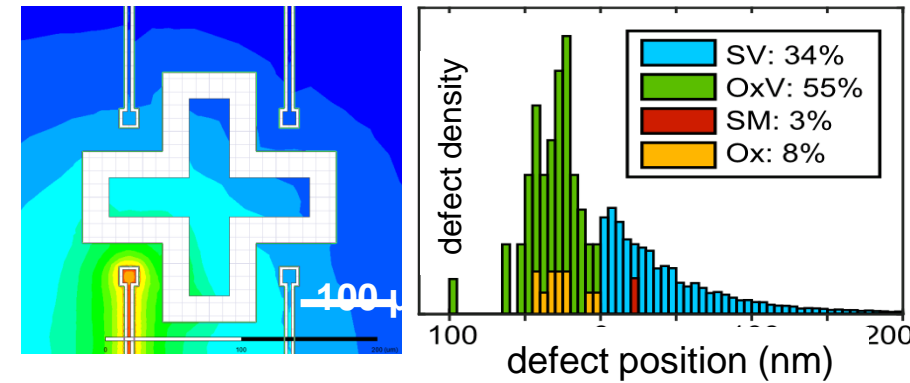
strain- & E-field spectroscopy



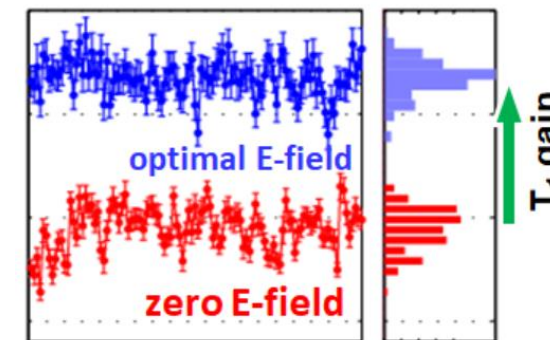
TLS-resonator coupling



mapping TLS positions



Improve qubit T₁ time



Google
Research

Baden-
Württemberg
Stiftung



Bundesministerium
für Bildung
und Forschung